Project BME-AJ1-1401

Microfluidic-based encapsulation of cells into microgel spheres

A Major Qualifying Project Report:
In partial fulfillment of the requirements for the
Degree of Bachelor of Science
Submitted to the Faculty of
WORCESTER POLYTECHNIC INSTITUTE
By:

_____
Arlina A. Anderson

_____
Marley G. Kapsimalis

_____
Kenechukwu M. Ndukwe

_____
Matthew H. Noyes

_____
Vincent A. Samuel

Date: April 30, 2015

Approved:

_____
Dr. Anjana Jain, Major

_____
Dr. Dirk Albrecht, Technical Advisor

Table of Contents

Table of Figures

Authorship Page

Section	**Author**
Abstract	A.A., V.S.
1 Introduction	All
2.1 Current Neural Stem Cell Treatments	K.N.
2.2 Mouse Stem Cells	A.A.
2.3 Fas and Anti-Fas	K.N.
2.4 Hydrogels	M.N.
2.5 Hydrogel Crosslinking Methods	M.N., V.S.
2.5.1 Michael Addition	M.N.
2.5.2 Photopolymerization	V.S.
2.6.1 Electrospray	M.K.
2.6.2 Microfluidic Devices	K.N. V.S.
3 Project Strategy	M.K.
4 Alternative Designs	K.N., V.S.
5 Design Verification	A.A., K.N.
6 Discussion	M.N
7 Conclusions and Recommendations	M.K

Acknowledgements

The team would like to thank the following people for their assistance on this project, without their help it would not have been possible:

- Dalia Shendi, for providing invaluable advice, knowledge, and assistance throughout the entirety of the project.
- Vicki Huntress and Katrina Hansen, for helping us image.
- Laura Aurilio, for her helping us create our silicone master.
- Benny Yin, Alex Believeau, and Kimberly Ornell for providing us with cells and answering our various lab questions.

Abstract

Stem cell-based therapy has shown great promise as a strategy to treat a number of neurodegenerative diseases and injuries (Lindavall et. Al., 2006). Neurodegenerative diseases refer to a range of different conditions that result from the death and/or degeneration of neurons (College, 2014). Some common neurodegenerative diseases include Alzheimer's disease, Parkinson's disease, Spinal Muscular Atrophy, Huntington's disease, Amyotrophic Lateral Sclerosis, and Spinocerebellar Ataxia (Medicine, 2000). However, currently only 5-10% of implanted neural stem cells (NSCs) survive the initial immune response. It has been demonstrated that transplanted NSCs encapsulated in hydrogel have a higher survival rate (Yang et. al., 2014). Therefore, a microfluidic device was designed to encapsulate live cells in microgel spheres;using a microfluidic device allowed for high-throughput encapsulation of the NSCs, as well as the production of uniform microgel spheres. Specifically, a flow-focusing microfluidic device was used for its ability to produce a more consistent microgel sphere size as compared to other devices, such as the T-junction. Hyaluronic acid (HA) was used as the encapsulating hydrogel. HA is a natural polymer found in the central nervous system (CNS) and has anti-inflammatory properties. Irgacure 2959 was chosen as the photoinitiator so that the microgel spheres could be photocrosslinked as they moved through the channels of the microfluidic device. Photocrosslinking of the HA was activated using an ultraviolet lamp. A protocol for cell encapsulation was developed in order to successfully encapsulate live cells in the microgel spheres. Once the protocol for microgel sphere formation was optimized, Jurkats cells, U87MG cells, or PC12 cells were cultured and were used to test for encapsulation within the microgel spheres. After collection of the spheres, they were stained with calcein and/or ethidium homodimer for cell viability analysis using a fluorescence microscope. The data collected shows that the developed system is able to create microgel spheres in the range of 50-70 μm that can encapsulate cells. However more testing is needed in order to validate the microfluidic design and encapsulation protocol. In addition, further optimization is suggested so as to improve the encapsulated cells' viability.

Chapter 1 – Introduction

Neurological diseases and injuries affect millions of people worldwide. Alzheimer's disease is the most common cause of age related cognitive degeneration and affects 12 million people worldwide, while Parkinson's disease affects 6 million people worldwide (Aarli et. al., 2006). Neurodegenerative diseases affect the metal ability of the patient to the point where it interferes with their daily life. Spinal cord injury (SCI) is a debilitating condition that affects millions of people worldwide and typically results in complete or partial paralysis. In the US alone, there are 12,000 new cases per year in addition to the 232,000-316,000 people already living with SCI (The National Spinal Cord Injury Statistical Center, 2011). These injuries are often irreversible and result from a variety of causes such as traffic accidents, acts of violence, falls, and sports injuries. Most SCIs occur when a fractured vertebra or disk intrudes the spinal canal, causing complete or incomplete severing of the spinal cord. While there are various degrees of contusion, laceration, and complete transection, the main issue associated with SCI is regeneration because the central nervous system (CNS) is not capable of spontaneous regeneration (Madigan et. al, 2009). The pathophysiology of SCI is unknown so current treatments, such as steroids, only address the symptoms of mechanical compression and acute inflammation without repairing the site of injury.

Current treatments for neurological diseases and injuries include drug therapy and stem cell therapy. Drug therapy is designed to target the various components of cognitive, memory, and movement disorders, while stem cell therapy is used to target injured tissue and promote functional recovery as well as preserve function in the brain and spinal cord (Aarli et. al., 2006). However, current pharmacological approaches are limited, as they offer transient benefits to the afflicted and

do not significantly modify the course of the condition. Stem cell therapies also have limitations, as proliferation and differentiation of the implanted stem cells into the desired cellular phenotypes must be controlled to prevent tumor formation. Furthermore, the mode of delivery affects the efficacy of stem cells to repair the damaged tissue. The mode of delivery is influenced by the pathological tissue environment, inflammatory, and immune reactions (Youdim & Buccafusco, 2005).

Only 5-10% of implanted stem cells survive the initial immune response. When foreign stem cells are implanted into a patient, the initial reaction of the body is to send T-Cells to the affected area. When T-Cells detect a foreign substance in the body, cytokines are released into the bloodstream to signal the presence of an unwanted body. Cytokine release triggers a cascade sending macrophages to the region, which destroy the foreign substance. Researchers need a way to prevent the body from destroying the implanted cells before they are able to integrate and become functional. The goal of this project was to design a microfluidic system that is capable of encapsulating mouse neural stem cells (NSCs) in biodegradable microgel spheres.

The project began with a literature review on microfluidic devices, microgel sphere generators, NSCs, hydrogels, immune response, and causes of damage to the nervous system. A set of design criteria was created from the client statement, client meetings, and the literature review. These criteria were further expanded upon and organized into constraints, objectives, functions, and specifications.

Initial designs were created in DraftSight and were based on the established constraints, specifications, and additional information provided by Professor Albrecht. The most important specifications taken into consideration when developing the initial device designs were microgel sphere size, channel size, and the number of cells per microgel sphere. By using these

specifications, the team was able to determine the proper channel width for optimum microgel sphere formation. The team used photolithography to make a silicon wafer as the master, which had the initial design options etched on. This silicon wafer was used as a template to transfer the designs to PDMS. The resulting PDMS microfluidic devices were tested to determine which designs generated microgel spheres that met the requirements and were fully crosslinked. The team picked the best design and developed a protocol for cell encapsulation. The microgel spheres were imaged to ensure that uniformly sized microgel spheres were formed and that the microgel spheres contained cells.

At the conclusion of this project, a protocol for cell encapsulation and a flow focus serpentine microfluidic device capable of producing microgel spheres within the desired size range (50-70µm diameter) was modified and developed. Although this system and corresponding protocols require further optimization and experimentation, it shows promise. Once optimized, this system can be applied not only to encapsulating NSCs for neurological cell therapy, but also to other cell types. This technology has the potential to revolutionize current stem cell therapy practices.

Chapter 2 – Literature Review

2.1 – Current Neural Stem Cell Treatments

Unlike most tissues in the body, the neural system has a limited capacity for self-healing. Neural cells have a limited capacity to regenerate and the small populations of endogenous NSCs in brain tissue are unable to fully reconstitute and restore function after damage. As such, research has gone into developing potential cell replacement therapies to treat cerebral injury. There are many proposed stem cell therapies designed to address various neurodegenerative diseases. In each of these diseases, a different spectrum of cell types is affected; therefore, different types of neurons are required for replacement. There are three main sources of cells for replacement: neural tissue from fetuses, immortalized cell lines, and embryonic stem cells. The main goal of these treatments is to promote survival and functional integration (Kennea, Weston Laboratory, Mehmet, Weston Laboratory, & Weston Laboratory, 2014).

Fetal neural cell transplantation has been used in several brain injury models to provide a source of immune-compatible cells for transplantation. One drawback is the supply of fetal neural tissue is limited and consequently only small numbers of neurons are available. This may be partially overcome by in vitro expansion. Immune rejection and subsequent failure of the graft can also be a problem, where there is poor graft survival and no clinical improvement. Lastly, there are ethical issues surrounding the use of fetal tissue, promoting the use of adult stem cells rather than those derived from fetal tissue.

Immortalized cell lines have been employed in animal studies of brain injury resulting in histological integration and functional improvement. Immortalized cell lines have been used to treat demyelinating diseases through the transplantation of oligodendrocyte progenitor cells

(OPCs) that migrate away from the injection site to repopulate areas of demyelination. However immortalized cell lines are prone to tumorigenesis and they are unable to reconstitute the wide variety of cell types lost in cerebral injury. This makes them of only limited use in clinical applications.

Embryonic stem cells are a promising alternative source of cells for therapeutic transfer. Embryonic stem cells are pluripotent, can be propagated in vitro, and can be engineered to express therapeutic genes. They can migrate and differentiate into regionally appropriate cell types, and do not interfere with normal brain development.

In some NSC treatments the stem cells are genetically modified with other substances to improve the efficacy of the therapy. In a treatment of intracranial glioma, NSCs are modified to secrete interleukin 12 (IL-12). Gliomas are difficult to treat because the tumor exerts immunosuppressive effects at both the systemic and local intratumoral levels. In addition, malignant gliomas are highly invasive, which provides them with the ability to infiltrate deep into normal tissue, establishing microscopic reservoirs from which regrowth can occur after surgical resection. IL-12 is a potent tumoricidal cytokine with demonstrated efficacy against intracranial glioma. The combination of IL-12 with the extensive migratory and tumor tracking characteristics of NSCs, results in a vehicle capable of delivering IL-12 to neoplastic pockets separate from the main tumor mass (Ehtesham et al., 2002).

2.2 – Mouse Stem Cells

2.2.1 – Differentiation Pathways

Mammalian NSCs are capable of differentiating and replacing neurons that are lost or injured due to trauma or disease. The differentiation of NSCs occurs in stages and is controlled by cues from the cell microenvironment.

All cells that make up the central nervous system (CNS) originate in the ventricular zone (VZ) from epithelial cells that have NSC properties. These cells are called neuroepithelial cells and are surrounded by extracellular matrix (ECM) molecules and signals, such as retinoic acid and fibroblast growth factors. These signals mediate cell-to-cell and cell-to-ECM interactions and trigger the neuroepithelial cells to divide in the VZ and form intermediate progenitors. Neurons are generated from the intermediate progenitor cells through neurogenesis. Neurogenesis occurs in two parts of the brain in adult mammals: the subventricular zone (SVZ) and the subgranular zone (SGZ). The SVZ lines the lateral ventricles of the brain and is where the intermediate progenitors divide symmetrically to produce neurons and glia. From the SVZ, new neurons, or neuroblasts, migrate to the olfactory bulb, a neural structure in the forebrain. The SGZ is a subunit of the hippocampus; neuroblasts that form in the SGZ are integrated into the hippocampal formation (Kazanis et al., 2008).

2.2.2 – Differences Between Neurons and Glia Cells

Mouse NSCs can be used to study the regeneration of neurons in humans. Neurons are electrically excitable cells that transmit signals to one another via synapses. Sensory neurons convey sensory information, such as feeling, to the brain or spinal cord. Motor neurons control

movement, and interneurons interconnect other neurons to form neural networks. On the other hand, glial cells are non-neuronal cells whose function is to provide support and protection for neurons and maintain homeostasis. The two types of glial cells that can differentiate from NSC are called astrocytes and oligodendrocytes (Purves et al., 2001). When transplanting NSCs into the body it is important to induce the right conditions for the desired type of cell to form, whether a neuron or a glial cell. One such condition is substrate or hydrogel stiffness. Researchers at the University of California Berkley discovered that optimal differentiation of NSCs into neurons occurred on substrates of intermediate stiffness and was approximately 500 Pa(Saha et al., 2008). The softer surfaces promoted neuronal differentiation while hard surfaces were found to favor glial differentiation (Banerjee et al., 2009). To ensure growth and renewal it is important to take precautions so that the cells survive the immune response that follows implantation.

2.2.3 – Stem Cell Death Pathway

The body's immune response can be broken down into several stages. The first stage is antigen recognition in which antigen-presenting cells (APCs), such as macrophages and dendritic cells, bind fragments of antigenic peptides from the donor cells. APCs then present these fragments to helper T cells through the T cells' antigen receptors. The APCs express major histocompatibility complex (MHC) molecules because the antigen peptides must be presented in conjunction with an MHC molecule for the T lymphocytes to recognize and destroy the antigen peptides. The APC can be an allogeneic or one of the body's own , autologous, depending on the donor cell death pathway. The activated helper T cells differentiate into effector cells and express cytokines and effector molecules on their membranes. When the cytokines or effector molecules are secreted, they act as growth and activation factors for cytotoxic T cells, B cells, and macrophages. The B cells mature

into plasma cells and secrete antibodies against the implanted cells, cytotoxic T cells trigger the apoptosis of the implanted cells, and macrophages initiate a delayed hypersensitivity inflammatory reaction (Sayegh & Turka, 1998).

Many treatments have been evaluated in order to suppress the immune response to donor cells. One way to achieve immunosuppression is by utilizing cells found in immune privileged sites in the body. Immune privileged sites can be exposed to antigens without eliciting an inflammatory immune response. As a result, NSC and other tissue grafts transplanted in immune privileged sites can survive for extended periods of time without rejection. Immune privileged organs are among the few cells in the body that express a protein called Fas ligand. Fas ligand protects cells in immune privileged sites from invading inflammatory cells and can increase the survival rate of transplanted NSCs post-implantation (Gregory et al., 2002).

2.3 – Hydrogels

Cells and tissue used in regenerative medicine need to grow into a structure suitable for replacing the damaged tissue in the body. Scientists have been designing scaffolds to encapsulate the cells to ensure that they properly grow into the body. Hydrogels provide many distinct advantages for developing the scaffold; they allow transplanted cells to be immunoisolated while still allowing nutrients, and metabolic products to diffuse into their matrices, and their mechanical characteristics can be tailored to mimic those of natural tissues. The process of encapsulating cells in the hydrogel is simple, and once encapsulated, the hydrogel can adapt to the surrounding tissue in the body. The injection of these hydrogels is a minimally invasive procedure that makes it easy to administer the hydrogel into the patient. However, there are complications associated with this procedure that can make this procedure difficult. There are very few chemical crosslinking systems

currently available that are biocompatible, and physical crosslinking methods are difficult to trigger. In addition, physically crosslinked hydrogels have low stability in the body. Once the cells are encapsulated, providing them with adequate growth factors can prove to be difficult (Yang et al.).

Despite these disadvantages, hydrogels are frequently used in tissue engineering for cell encapsulation purposes. The properties offered by hydrogels make them an excellent choice in material for cell encapsulation. Hydrogels have excellent permeability, which allows for the diffusion and transport of essential materials, such as oxygen and nutrients. Numerous biodegradable hydrogels have been developed for usage in drug delivery and cell scaffolding. Due to the three dimensional network structures of the hydrogels, and their viscoelasticity, hydrogels are useful scaffolds, allowing for cell adhesion, cell spreading, and cell proliferation. In addition, there is a lot of promise in the usage of hydrogels for the repair and regeneration of various tissues and organs (Yang et al.).

2.3.1 – Factors in Hydrogel Selection

When selecting a hydrogel for cell encapsulation, there are a number of factors that must be considered. These considerations are necessary to ensure that the cells survive the encapsulation process and continue to survive once encapsulated. The process of encapsulation or the transition of the solution from liquid to hydrogel must not place undue stress on the cells. Once the cells are encapsulated in the hydrogel, the structure of the hydrogel must allow cell growth and the hydrogel must properly degrade to allow the tissue to form. Other key factors that must be considered are

the products formed by the hydrogel upon degradation. Degradation products must be nontoxic and biocompatible, both to the cell culture and the patient (Nicodemus & Bryant, 2008).

In addition, the liquid precursor solution used to suspend the cell culture must meet certain requirements as well. The components must be water soluble, as to properly mix with the cell solution. This solution must also be buffered with salts to prevent cell lysis within the solution (Nicodemus & Bryant, 2008).

2.3.2 – Alginate

Alginate is a polysaccharide containing a mixture of β-D-mannuronic acid and α-L-guluronic acid. Alginate hydrogels are formed through ionotropic crosslinking, a process that is gentle on the cells and reversible. Some previous applications of this hydrogel have been found in wound dressing and food additives, but it has also shown a lot of promise in cell encapsulation. Alginate hydrogels have previously been used to encapsulate dorsal root ganglia and neural progenitor cells (Hunt & Grover, 2010).

2.3.3 – Collagen

Collagen is a protein found in almost all animals. It is the main structural protein that makes up connective tissues in animals and up to 30% of the total protein content in humans. By dispersing collagen in an acid, and then neutralizing it, one can form a collagen-based hydrogel that has a very high cell adhesion. Another appealing property of collagen-based hydrogels is that type I collagen hydrogels are able to self-assemble. The two major drawbacks to using collagen

based hydrogels is that they have weak mechanical properties and they contract when used to encapsulate cells (Hunt & Grover, 2010).

2.3.4 – Fibrin

Fibrin is a naturally occurring protein in the body that is used to form blood clots during wound closure. Fibrin gels form by proteolytic cleavage, caused by interaction with thrombin, exposing various regions on the protein that allow it to self-assemble. Fibrin gels are useful for cell encapsulation because they have regions that enable both cell adhesion and growth factor binding. The major drawback of these gels is that they rapidly degrade when encapsulating mammalian cells, due to the proteolytic enzymes that the cells secrete (Hunt & Grover, 2010).

2.3.5 – Gelatin

Gelatin is a molecule formed from the hydrolysation of collagen. Gelatin can be used to form hydrogels by dissolving the molecule into water at 60 °C, and then cooling to room temperature. Previous cell encapsulation experiments done with gelatin have been done for the encapsulation of chondrocytes and hepatocytes, cells from the cartilage and liver, respectively (Hunt & Grover, 2010).

2.3.6 – Hyaluronic Acid

Hyaluronic acid is a derivative of hyaluronan, a polysaccharide found through the body in the skin and cartilage tissues, among others. Hyaluronic acid is naturally found in the central

nervous system and is anti inflammatory. By modifying hyaluronic acid with thiols, methacrylates or tyramines the molecules can be chemically crosslinked to form a hydrogel. One of the key advantages of using hyaluronic acid is that the degradation of the hydrogel can be moderated by hyaluronidase, an enzyme secreted by a multitude of mammalian cells. These hydrogels have also been used for the encapsulation of dorsal root ganglia, a neural cell (Hunt & Grover, 2010).

2.3.7 – Hydrogel Mixes

Many hydrogels are not made exclusively from a single type of polymer. Often the case is that the properties of the hydrogel can be improved by mixing multiple different polymers together to get a different type of hydrogel. Often the components are selected to complement each other's properties. Below are two examples of hydrogels formed by fusing different compounds.

2.3.7.1 – Chitosan-Gelatin

One popular hydrogel that is formed by combining different polymers is formed by mixing chitosan and gelatin. Chitosan is a deacetylated version of chitin, a protein that is found in the exoskeletons of insects and crustaceans. Structurally, chitosan mimics hyaluronic acid, which is a crucial component of the extracellular matrix. Chitosan has been shown to be blood compatible, and is used extensively in biomedical science. The chitosan-gelatin mix has been shown to be biocompatible and immunocompatible as well, when tested against macrophages (Risbud, Endres, Ringe, Bhonde, & Sittinger, 2001).

2.3.7.2 – Alginate-Chitosan

Another popular hydrogel used for cell encapsulation is formed by a mixture of alginate and chitosan. Many different reactions are possible to form this hydrogel; in this paper two will be covered. The single stage procedure involves suspending the cell culture in 1.2% sodium alginate solution at a cell density of 1 X 10^6 cells/mL. The solution is then pushed through a microgel sphere forming device into a chitosan solution where they are allowed to form into a gel. The two stage procedure is similar to the single stage procedure, in which only the alginate is pushed into a calcium chloride solution for gel formation, and the microcapsules are reacted with chitosan to form a coating around them (Baruch & Machluf, 2006).

2.4 – Hydrogel Crosslinking Methods

The formation of a hydrogel occurs due to crosslinking between the individual polymer chains that make up the precursor of the polymer. During the crosslinking process, the polymer chains are connected by covalent, ionic, or physical bonds. These changes alter the physical state of the solution, changing it from a liquid to a gel state (Nicodemus & Bryant, 2008).

Typically cells are suspended in a solution containing a gel precursor. This precursor must be water soluble, and buffered appropriately to prevent cell lysis. From here, the hydrogel is formed using radical chain polymerization or chemical crosslinking. These methods are used to generate covalently crosslinked hydrogels. Radical chain polymerization occurs when an initiator is present. The initiator reacts with the polymer to generate a free radical that moves through carbon-carbon double bonds to form covalently bonded chains.

Chemical crosslinking methods have also been employed to encapsulate cells. These methods do not always require the presence of an initiator, though some require a precursor to

catalyze the reaction. There are many different chemical reactions used to form hydrogels, such as the well-known Michael Addition reaction.

Crosslinking refers to the process of chemically joining two or more molecules by a covalent bond. Crosslinking reagents are molecules that contain two or more reactive ends that have the ability to chemically attach to certain functional groups on other molecules or proteins.

The type of crosslinker chosen depends on their specificities for particular functional groups as well as other chemical properties that affect their behavior. The first property to consider when choosing a crosslinker is the crosslinker's chemical specificity. Chemical specificity refers to the reactive ends of the crosslinker, and whether or not they are homobifunctional or heterobifunctional. Homobifunctional crosslinkers are molecules where the reactive ends are identical, whereas heterobifunctional crosslinkers have different reactive ends. It is also important to look at the spacer arm length of the crosslinker. The spacer arm length refers to the distance between conjugated molecules. The water solubility and permeability of the cell membrane of the crosslinker is important because it determines whether or not the crosslinker can permeate into cells as well as crosslink hydrophobic proteins within membranes. Lastly one should look at the spontaneously reactive or photoreactive groups in a crosslinker. This determines whether the crosslinker will react when it is added to a sample or if it can be activated through exposure to UV light (Hayworth, 2014).

2.4.1 – Michael Addition

Michael addition is a chemical crosslinking procedure that involves the addition of a carbanion or a nucleophile, such as a thiol or amine, to an unsaturated carbonyl compound. This procedure has previously been used to create PEG, collagen, heparin, and hyaluronic acid

hydrogels. When used in cell encapsulation, the procedure is as simple as suspending the cell culture in the polymer solution, and adding the precursor. Hydrogels such as Extracel have been formed by this method and are used in tissue engineering and drug delivery applications (Yang et al.).

2.4.2 – Photopolymerization

There are two types of polymerization, step-growth polymerization and chain-growth polymerization. Step-growth polymerization is a type of polymerization where bi-functional or multi-functional monomers react to form first dimers, then trimers, then oligomers, and eventually long chain polymers. Chain-growth polymerization is the linking of molecules that incorporate double or triple carbon-carbon bonds. The monomers polymerized through chain-growth polymerization have the ability for their bonds to break and link with other monomers to create a chain (Stille, 1981). A type of chain-growth polymerization is photopolymerization. Photopolymerization occurs when visible or UV light interacts with light sensitive photoinitiators to create free radicals that initiate polymerization. Photopolymerization allows for spatial and temporal control of polymerization. It also allows for fast curing rates ranging from a few seconds to a few minutes at normal temperatures with little heat production. In terms of hydrogels, photopolymerization is minimally invasive to the hydrogel and therefore preferred (Nguyen & West, 2002).

2.5 – Methods and Devices for Microgel Sphere Generation

2.5.1 – Electrospray

Electrospraying is one of a few methods used to generate microgel spheres from various liquids and solutions, including cell suspension inside a hydrogel, in the micro to nano range (Young, Poole-Warren, & Martens, 2012). There are two variations of electrospray, electrospray in air and submerged electrospray (Young et al., 2012).

Electrospray in air uses a capillary or needle, an electric potential, and a surface to create microgel spheres. A potential difference is created between the needle and a grounded electrode, charging the liquid in the needle (Hager & Dovichi, 1994; Suwan N Jayasinghe, Qureshi, & Eagles, 2006; Workman, Tezera, Elkington, & Jayasinghe, 2014). The flowing liquid exits the needle in a thin jet and disperses as it passes through an electric field, see Fig 3.a (Hager & Dovichi, 1994; Suwan N Jayasinghe et al., 2006). Since the microgel spheres have the same charge they quickly separate and land on the designated surface. Microgel sphere size is controlled by flow rate, potential difference, and the liquid properties, such as viscosity (Workman et al., 2014). Electrospray in air has successfully been used to encapsulate cells in a synthetic hydrogel that caused no adverse effects to the cells in both blood monocyte and neuronal cell lines (Hager & Dovichi, 1994; Suwan N Jayasinghe et al., 2006). The cells showed no changes in shape, no alterations in mitosis, or other damage (Suwan N Jayasinghe et al., 2006).

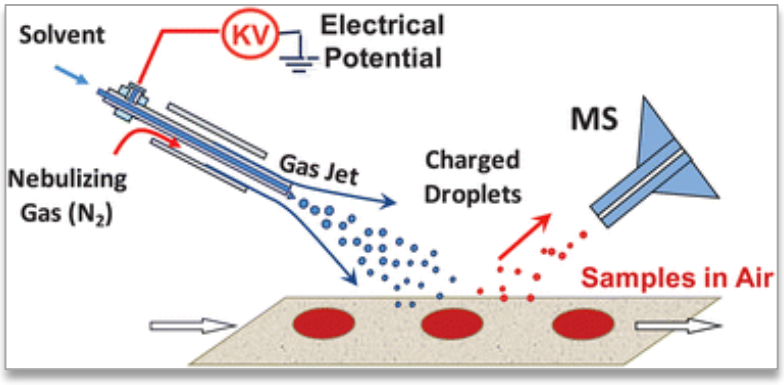

Fig. 3.a – Typical electrospray in air set-up (Ifa, Wu, Ouyang, & Cooks, 2010).

Submerged electrospray is similar to electrospray in air, except the microgel spheres are dispersed in an insulating liquid instead of in air or a vacuum. This method of electrospray utilizes a syringe pump, a needle, an electric potential, an earth electrode, a UV light source, and an insulating liquid, specifically sunflower oil and surfactant, see Fig 3.b (Young et al., 2012). Similarly to electrospray in air, the charged liquid flows through the needle and exits in a jet. The earth electrode causes the jet to disperse microgel spheres into the insulating liquid. The microgel spheres are then polymerized by the UV light. Microgel sphere size is controlled by flow rate, potential difference, and the liquid properties. Submerged electrospray has successfully encapsulated cells in synthetic hydrogels with high viability (Young et al., 2012).

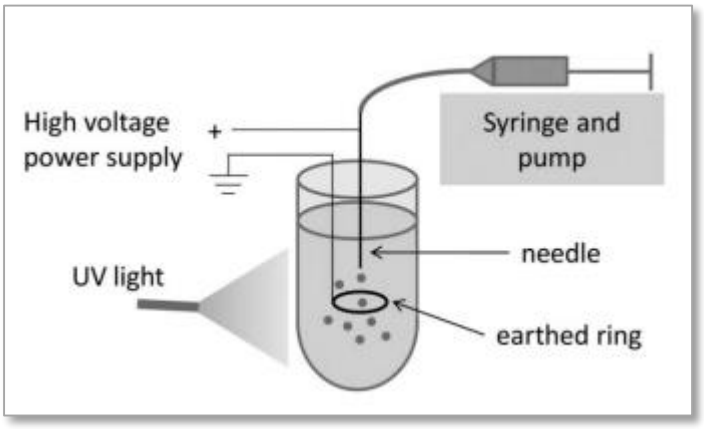

Fig. 3.b - Submerged electrospray schematic (Young et al., 2012)

While the method of electrospraying liquids is well established, electrospraying cells is relatively new and has a few issues in need of solutions. A common issue with electrospraying of cells is its inability to evenly disperse cells within the microgel spheres, resulting in uneven nutrient absorption (Suwan N. Jayasinghe, 2011). Another issue, specifically for encapsulation of cells, is unstable jetting conditions caused by ion uptake in cells (Suwan N. Jayasinghe, 2011). Electrospraying is a viable option for cell encapsulation in a hydrogel but further research has to be conducted to resolve these issues and fully understand the effect on cells at a molecular level (Suwan N. Jayasinghe, 2011; Mongkoldhumrongkul, Swain, Jayasinghe, & Stürzenbaum, 2009).

2.5.2 – Microfluidic Devices

Microgel sphere formation and size in microfluidic devices can be determined by controlling the geometry of the outlet and of the channel junctions. A microfluidic device can be designed with an expanding nozzle and/or T-junctions in the microfluidic channels. The expanding geometry in the nozzle would create a velocity gradient that precisely dictates the breakup location of the liquid thread, thereby allowing for control over the microgel sphere generation positioning and the breakup location of the microgel sphere. Microgel spheres are generated in T-junctions by controlling the inlet pressure or by dictating a constant flow rate using a pump. A drawback of using T-junctions is microgel sphere non-uniformity and instability (Piotr, Michael, Howard, & George, 2006) .

Microgel sphere formation and size in microfluidic devices can be controlled by a piezoelectric actuator and/or electrostatic forces. A piezoelectric actuator can be used to convert electric voltage into mechanical translation to create a constant flow rate at the inlets, thereby enabling stable single microgel sphere formation. This method is useful for microgel sphere based micro-devices requiring synchronization and on demand generation. In addition, an electrostatic force can be used to generate microgel spheres. In this method, a high electric field pulse is applied on an oil-water interface, which charges the interface and causes microgel sphere formation. However this method is impractical for low cost simple devices and is unsuitable for cell encapsulation or diagnosis (Bransky, Korin, Khoury, & Levenberg, 2009).

2.5.2.1 – Microgel sphere Formation

The most common method for microgel sphere formation is through emulsion of two immiscible phases. Oil and water are common examples of this. Different types of oil phases are

commonly used. Hydrocarbons, silicones, and fluorinate oils are examples of different oil phases that can be used. Some examples of Hydrocarbon oils are hexadecane, vegetable oil, and mineral oil. Hydrocarbon oils are easily attainable and cheap, but are not usually compatible with cells. Silicone oils are also not a great option because they are not compatible with Polydimethylsiloxane (PDMS), which is a very common material for microfluidic devices. Fluorinate oils are the best option because they are biocompatible but are very expensive (Baret, 2012; Teh, 2008).

One does not necessarily have to use the oil phase; there are other aqueous phases that can be used. The important factor is that the phases are immiscible. It may be necessary to add surfactants to whatever phase is used in order to prevent the microgel spheres from coalescing or combining. Surfactants prevent the microgel spheres form combining by providing an energy barrier that stabilizes dispersion. Surfactants stabilize dispersion through steric repulsion of the surfactant molecules or surfactant gradients at the interface of the microgel spheres. The surfactant gradients at the microgel sphere interface results in what is referred to as the Marangoni effect. The Marangoni effect is when the surfactant distribution is non-uniform and leads to a gradient in surface tension, which creates a stress that opposes the flow (Baret, 2012).

The common and easiest method to form microgel spheres is when the dispersed phase is flowed through a microchannel as the flow from the immiscible liquid is independently flowed through a separate microchannel. These two phases end up meeting at a junction and shear stresses at the interface cause microgel spheres to form. Flow-focusing junctions as well as T-junctions are both designs used to facilitate the formation of microgel spheres. In the flow-focusing designs both phases are flowed through a narrower region where constriction allows for symmetric shearing which generates microgel spheres. In T-junctions an inlet channel containing one phase intersects a main channel that contains the other phase. Once they intersect shear forces and pressure

gradients force the inlet channel phase to elongate and eventually break into a microgel sphere. Changes to flow rates, channel dimensions, and relative viscosities can all alter the microgel spheres in terms of size and frequency (Teh, 2008).

2.5.2.2 – Flow Control

There are a couple of flow control methods that could be used for the microfluidic devices. The first method is through hydrostatic pressure. Hydrostatic pressure involves a reservoir, a priming syringe, a 3-way valve and tubing for the inlets and outlets of the microfluidic device. Hydrostatic pressure uses gravity to control flow. Some advantages to using hydrostatic pressure are that it is cheap and easy to set up, and its efficacy is easily altered by simply raising and lowering the height of the reservoirs. A disadvantage to hydrostatic pressure is that if the reservoirs are not monitored the flow may change. Another method of flow control is by using a syringe pump. Syringe pumps are useful because they are controlled by a computer and result in direct flow rate control. Some negative aspects of using a syringe pump is that it takes a considerable amount of time to maintain the flow rates desired and it also has a slow response to flow rate changes, so it is only useful for long periods of flow control. (Albrecht, 2014).

Chapter 3 – Project Strategy

The primary goal of this project was to design and fabricate a microfluidic device for NSC encapsulation. The purpose of this chapter is to explain the identified objectives and constraints associated with various components of the project. The initial client statement was revised after the group evaluated the objectives and constraints.

3.1 – Client Statement

Professor Jain, the client, provided the following client statement to the team:

To design and fabricate a microfluidic device that encapsulates neural stem cells in a biodegradable hydrogel capable of modulating the immune response to increase transplanted neural stem cell survival.

After further research and discussion with Professor Jain, the team revised and refined the initial client statement to the following:

Design and fabricate a microfluidic system that encapsulates neural stem cells in a biodegradable hydrogel capable of modulating the immune response to increase transplanted neural stem cell survival.

The revised client statement was broken down into two main project aims:

1. Design a microfluidic device that is capable of encapsulating mouse neural stem cells in biodegradable hydrogel microspheres
2. Minimize the initial foreign body response of T-cells towards implanted neural stem cells

3.2 – Objectives

The client statement was broken down into three main project aims:

1. Determine the hydrogel composition
2. Determine and test photopolymerization mechanisms
3. Design microfluidic devices using DraftSight®

The team determined the hydrogel composition first because viscosity is a major determinant of the device design with respect to the channel dimensions. The team researched the various hydrogel options and discussed them with Professor Jain to determine the best option. In addition to the hydrogel composition, the team determined the photopolymerizer as this effects the composition of the hydrogel and the length of time required to crosslink the hydrogel, ultimately affecting the geometry of the device. The team conducted a research and discussion process similar to that used for the hydrogel to determine the best photocrosslinker. The team broke down the third project aim, design a microfluidic device, into a series of primary and secondary objectives as seen in Fig. 4.

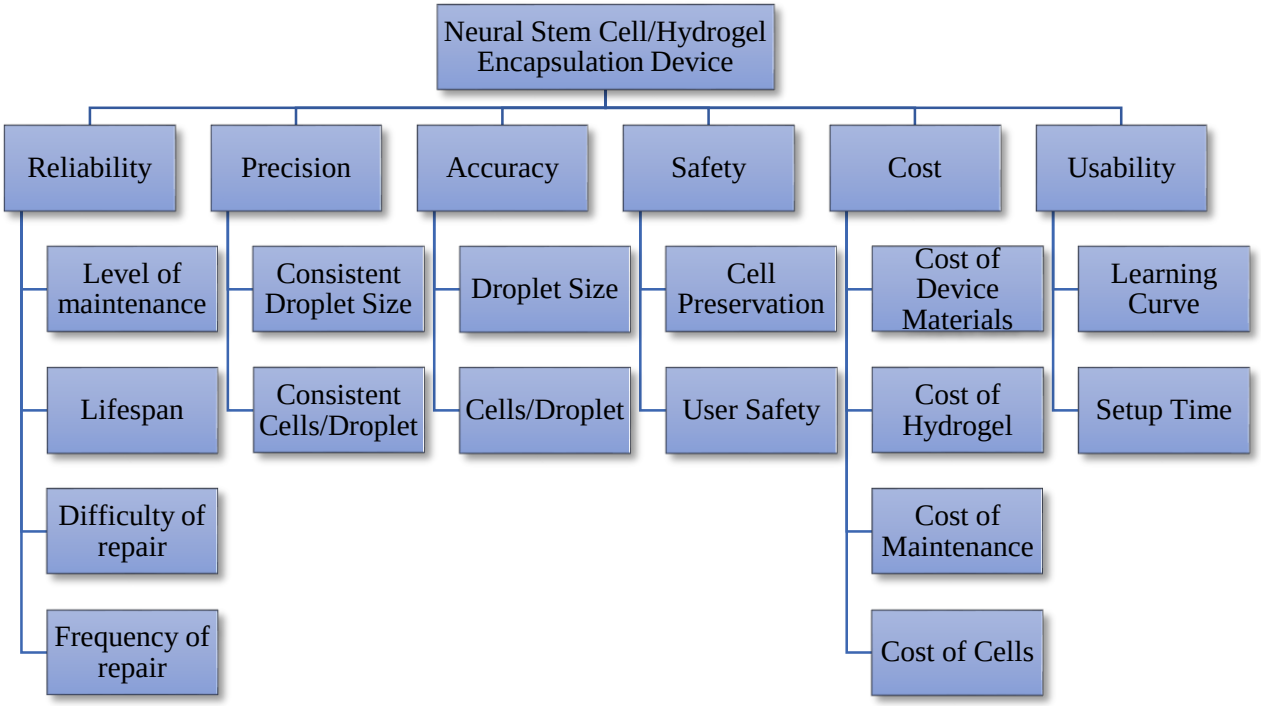

Fig. 4. Design Objective Tree

The team needed to create a device that was reliable, precise, accurate, safe, usable, and had a reasonable cost.

Reliability: The device would be used in lab by Professor Jain and had to be reliable. Reliability included a minimal level of maintenance, a reasonable lifespan, and easy and infrequent repairs. The time required to make the device had to be less than the total amount of time it was used in lab. The repairs had to be simple and replacement parts should be easily obtained, either commercially or in lab.

Precision and Accuracy: The device had to be both precise and accurate so that the client would know the number of NSCs delivered in order to alter doses and accurately determine the interaction between the injected NSCs and the surrounding area, as well as the effect the NSCs would have on the surrounding area. A device that created uniformly-sized microgel spheres would help to evaluate the number of NSCs delivered. .

Safety: In terms of safety, the device had to be safe for the user to use as well as safe for the cells. User safety meant that no additional safety precautions were required outside of standard lab protocols when using the device. Cell safety meant that cells survived encapsulation and were not altered during the encapsulation process. All chemicals, light wavelengths, hydrogel viscosity and stiffness, and shear stresses had to be conducive to mouse NSC survival.

Cost: The final cost of the device needed to remain low so that upkeep, maintenance, and replacement of supplies was feasible within Professor Jain's working budget. Hydrogel and cell sources needed to be those already in Professor Jain's lab.

Usability: The last secondary objective was usability. The device setup needed to be quick and simple to learn, as the device would serve as tool in Professor Jain's experiments and would not be the focus of the experiments.

Professor Jain expressed that; precision, accuracy, cell safety, and usability were the top priority.

3.3 – Constraints

The team identified a series of constraints that the design could not violate based on the client statement and meetings with the client.

- Time
- Hydrogel source and type
- Cell type
- Device design
- Cost

The first constraint was that the team had to design, construct, and test the device within one academic school year. Hydrogel options were constrained to those currently available in Professor Jain's lab, such as collagen, chitosan, and hyaluronic acid.

In addition to the above constraints, the design of the device had several constraints in order to produce a useable product. The channels of the device designs had to be greater than 50 µm wide to prevent particulates and dust from clogging the channels and disrupting flow. The channels had to be more than 100 µm apart in order to prevent leakage of the fluid. The inlets had to be 1 mm circles, spaced more than 2 mm apart, allowing the tubing to be easily inserted into the device. To allow for error when cutting out the PDMS, 3 to 4 mm of space had to be left around the edges of the device design, inlets, and outlet. There had to be a 5 mm border around the edge of the 4 in silicon wafer because spin coating leaves a thick layer of photoresist at the edge of the wafer. The thick layer is not exposed to the proper light intensity during the photolithography process, causing designs in those areas to not sufficiently imprint onto the wafer. Financial constraints and considerations are discussed in Section 3.4.

3.4 – Financial Considerations

The team had a budget of $780 provided by Worcester Polytechnic Institute (WPI). The client expressed that additional money was available if she deemed the purchase necessary. The majority of the team's WPI budget was used for purchasing the photocrosslinker, components for photolithography, and printing the photomask.

Photomask printing cost about $135 and the Irgacure photocrosslinker cost around $85/kg. The remainder of the budget was used for silicon wafers, tubing, syringes, and other supplies necessary for the construction of the device.

3.5 – Project Approach

The goal of this project was to design and fabricate a microfluidic system that was capable of encapsulating cells. In order to do this, the literature was reviewed to determine which materials and device designs would be appropriate for use in this project. Experimental procedures determined which device was best to use, based on crosslinking time and the occurrence of microgel sphere coalescence. Further experimentation was used to refine the encapsulation protocol. Finally, fluorescence and bright field microscopy in combination with live/dead staining were used to evaluate the microgel sphere size distribution and cell encapsulation.

There were some technical challenges that had to be overcome throughout this project. The first challenge was the team's inexperience with microfluidics. The team had to learn the approach and techniques required to successfully design a microfluidic system. Equipment availability due to other researchers contributed to imaging delays. The major technical issue the team faced was device troubleshooting. During the experimental process, the device would clog either in the inlet because of premature hydrogel crosslinking or in the channels due to large Irgacure particles blocking channels. When the device clogged, the process had stop and restart so the device could be cleaned. This occurred frequently caused delays of up to an hour, or in some cases the device could no longer be used and the experiment had to stop until a new device was made.

Chapter 4 – Alternative Designs

4.1 – Needs Analysis

Stem cell-based therapy has shown promise in treating different neurological disorders and injuries. Unfortunately only 5-10% of implanted NSCs survive the initial immune response. Transplanted NSCs that are encapsulated in a hydrogel have a higher survival rate. The use of microfluidics allows for encapsulation of NSCs in a hydrogel.

In order to effectively encapsulate NSCs in microgel spheres through microfluidics, many different design alternatives were created and evaluated. In order to evaluate these design alternatives, the functions and specifications were analyzed to determine the most effective design.

In order for the encapsulation of NSCs in microgel spheres to be effective it needed to satisfy the needs of the client, which were as follows:

Reliability: The device had to require a minimum level of maintenance and a reasonable lifespan with infrequent repairs.

Precision and Accuracy: The device had to be both precise and accurate so that the client could know the number of NSCs delivered in order to alter doses and accurately determine the effective therapeutic dose. Creating spheres of uniform size capable of encapsulating a consistent number of NSCs was also necessary.

Safety: The device had to be safe for the user and safe for the cells. Therefore, the use of the device could not require additional safety precautions outside of standard lab protocols to be taken and cells had to survive the encapsulation process.

Cost: The upkeep, maintenance, and replacement of supplies for the microfluidic device had to be feasible for Professor Jain's lab budget. It was thus preferred that hydrogel and cell sources be chosen from those already available in Professor Jain's lab.

Usability: The setup for the experimental process of encapsulating NSCs through the microfluidic device had to be user-friendly.

4.2 – Functions

To achieve the objectives specified by the client for this project, this project needed to achieve two main functions. The first main function of this project was the formation of microgel spheres used to encapsulate cells. The device used needed to be able to generate a steady stream of microgel spheres at a consistent size and diameter. Consistency between the microgel spheres was important for the therapeutic aspect of the project.

The second main function of our device was crosslinking of the microgel spheres so that they maintain their shape upon removal from the device. In order to test these functions, the microgel spheres were observed under a fluorescent microscope. Two items were looked for during these tests. First, the group looked for the presence of fully formed microspheres, observed as dark circles in the solution. The second element the group looked for in the solution was the presence of cells within the microgel spheres. Observing cells under the microscope required the usage of fluorescent tagging in the cells prior to encapsulation. The group looked for the presence of fluorescent cell markings within the boundaries of the microspheres.

To achieve the formation of microgel spheres the group decided to use a microfluidic microgel sphere generator. More specifically the group used a flow focusing device, which creates microgel spheres by directly injecting the discrete phase containing HA and cells into the

continuous phase containing the oil, surfactant, Irgacure, and solvent blue. Microgel spheres are formed through the compression of the discrete phase by the continuous phase.

To achieve crosslinking, our group chose to use ultraviolet light crosslinking as our method for hardening the microgel spheres. HA does not naturally crosslink by exposure to ultraviolet light. This effect is obtained by adding Irgacure into the solution, which stimulates crosslinking.

The primary alternative that was considered for the crosslinking step was to use a chemical crosslinker in our device. Alternatively, our group looked into the application of a Michael addition reaction to crosslink the microgel spheres. The group decided to use photocrosslinking over chemical crosslinking because photocrosslinking allowed for better control over when crosslinking of the spheres occurred.

Ultraviolet crosslinking poses a risk of cytotoxicity to the cells. The ultraviolet light can kill the cells if they are exposed to the light for an excessive amount of time. However, the cells exposure to ultraviolet light was limited to increase the cell viability. In addition, the Irgacure crosslinker the team added to the HA proved toxic to the cells. The cytotoxic effects of the Irgacure were minimized by adding the Irgacure to the continuous phase solution instead of including it in the discrete phase solution, separating it from the cells.

4.3 – Conceptual Designs

The microfluidic chip the team used was made out of a polymer called polydimethylsiloxane (PDMS). There are multiple advantages to using PDMS for our microfluidic chip. PDMS allows for the ability to observe activity in the micro-channels under a microscope because it is transparent at a wide range of optical frequencies, 240nM-1100nM. Next PDMS has a low autofluorescence making it a common polymer used in microfluidics involving photo-

crosslinking. Also PDMS is easy to mold, allowing it to mold structures as small as a few nanometers. (PDMS: a review, 2015)

In terms of microfluidics there are two broad classes of microfluidic devices. The two classes of devices are t-junctions and flow focusing nozzles. Both of these classes have the capability to generate monodisperse particles as well as form emulsions of different sizes. As you can see in Figure 5 below, a represents the T-junction class, and b represents the flow focusing junction class. In the T-junction the continuous phase is met by the discrete phase perpendicularly. With the flow focusing junction, the discrete phase is injected in between the continuous phase. (The role of feedback in microfluidic flow-focusing devices, 2015) Looking at studies done with both the t-junction and flow focus junction, the team found that the flow focusing junction would be more beneficial to this project. There are a couple of advantages to using the flow focus junction over the T-junction. The first being it has been seen that the flow focus junction produces a more consistent emulsion size than the T-junction. Another advantage to choosing the flow focus junction was because numerous studies involving microfluidics using photo-crosslinking.

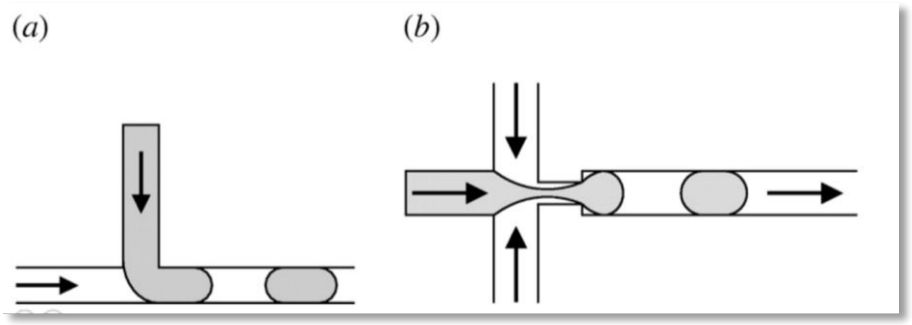

Fig. 5. A) T-junction device B) Flow-focusing device

Using a photoreactive group as the crosslinker in our gel allowed for immediate hardening of the gel once it would be exposed to ultraviolet light once the microgel spheres were formed. (Hayworth, 2014)

When looking at flow control there were two options available to us in our lab, hydrostatic pressure and syringe pumps. Hydrostatic pressure uses a difference in reservoirs to use gravity force to move the fluid from the inlet to the outlet. This method is useful for short periods of time because as the inlet reservoir is emptied and the outlet reservoir is filled the pressure difference changes. On the other hand, syringe pumps are perfect for low control over longer periods of time. The only drawback for our use of the syringe pump is that it takes 10 to 15 minutes for the syringe pumps to reach flow it is set to. Syringe pumps control the flow rate independent from fluidic resistance (Flow control in microfluidic devices, 2015).

4.4 – Design Alternative Evaluation

Throughout the experiment alterations were made in order to optimize the protocol to better create microgel spheres that encapsulated cells. At first, HA was dispersed with Irgacure 2959 into well plates at different concentrations and exposed to UV (365 nm wavelength and 3.8 mW voltage) in order to observe when and if crosslinking of the gel would occur. After repeated experimentation, it was found that crosslinking of the HA occurred when the HA and Irgacure was pre-mixed and small amounts of the mixture was exposed to UV. HA was used as the hydrogel because the experiment laid the basis for a system that delivers NSCs to traumatic injury sites such as the brain. HA is a natural polymer found in the CNS with similar mechanical properties to brain tissue. HA also has anti-inflammatory properties, making it better fit for the experiment when compared to other natural polymers such as chitosan and alginate. Photocrosslinking was used

instead of chemical because the catalysts used in chemical crosslinking can be toxic to cells. Irgacure 2959 was used as the photoinitiator because it is highly efficient and is especially suited for use in acrylate-based systems. Although Irgacure is cytotoxic, it is less so than the chemical crosslinking catalysts.

There were several device design options to choose from. Both T-junction and flow-focus devices were suitable for the experiment because they have the capability to generate monodisperse particles and to form microgel spheres of different sizes. Between the two, a flow-focus device was used because flow-focusing devices have been shown to produce a more consistent microgel sphere size (Casquilas, 2015). Several flow-focus devices were used in testing: a straight-channel device with a collection chamber, a straight-channel device with no collection chamber, a serpentine device with a collection chamber, and a serpentine device with no collection chamber. The device that best suited the experiment was the serpentine device with no collection chamber. Its longer channel length allowed for the microgel spheres to have extended UV exposure for crosslinking. Having no collection chamber reduced the risks of the spheres coalescing.

All of the design parameters were chosen with the goal of creating microgel spheres between 50 and 70 μm. This size was desired so that multiple cells could be encapsulated in a single sphere. Two solutions were pumped into the microfluidic device: an oil mixture and a hydrogel mixture. At first the oil mixture contained mineral oil and 2% Span 80 surfactant. The surfactant was used to prevent coalescence. The hydrogel mixture contained 0.75% HA, 0.5% Irgacure, and cells. After experimentation, the Irgacure was moved to the oil mixture to reduce the cytotoxicity to the cells, the volume percent of Span 80 was increased to 5% because coalescence of the spheres was observed with 2% Span 80, and dye was added to the oil mixture to help with visualization. Solvent blue was used as the dye because it completely dissolves in solution unlike

other dyes that can form particles in solution. The final mixture components were mineral oil, 0.5% Irgacure, 5% Span 80, and 0.05% Solvent Blue for the oil and 0.75% HA and cells for the hydrogel mixture.

Many flow rates were tested in order to find the rates that induced sphere formation of the desired size. By experimenting with different flow rates, it was found that setting the flow rate of the HA to 25 μl/hr and the flow rate of the oil to 50 μl/hr produced microgel spheres, however the spheres were larger than desired. It was later found that a flow rate of 250 μl/hr for the oil mixture and 50 μl/hr for the hydrogel mixture created spheres in the correct size range.

In order to confirm that the size of the microgel spheres was in the desired range, a size distribution was created by measuring and plotting the microgel sphere sizes of 360 spheres. The size distribution, shown in Fig. 6, displayed that most of the microgel spheres were in the desired range. In addition, the average sphere diameter was calculated to be 64.9 ± 6.4 μm, which was within the desired sphere size of 50-70 μm.

Two different methods of exposing the microgel spheres to UV were executed in order to determine the best way to crosslink the microgel spheres. One method used a platform UV lamp and the other used a handheld UV lamp, both with a 365 nm wavelength and 3.8 mW voltage. It was found that when the device was put under the beam of the handheld UV lamp, crosslinking occurred. This technique was later revised to the device being taped down on top of the handheld UV lamp so that the channel of the device had more direct exposure to the UV.

After flow rates that produced microgel spheres were found, cells were added into the HA to test if the cells could successfully be encapsulated in the microgel spheres. Three different cell types were used: Jurkats, pc 12, and U87MG cells. The cell types were used due to the fact that they were readily available. Jurkats had the added benefit of being easy to culture and U87MG

cells, a type of green-fluorescing protein, simplified the visualization of cell encapsulation by fluorescing green. After collecting the microgel spheres, live/dead staining was performed, and fluorescence and brightfield microscopy was performed on a section of the collection. The Jurkats and pc 12 cells were stained with calcein, a stain that stains live cells green, and ethidium homodimer, a stain that stains dead cells red. The U87MG cells were stained only with the ethidium homodimer. Fig. 7. is an image of cell encapsulation within a microgel sphere. An overlay of fluorescent live and dead U87MG cells with the brightfield image is shown. Dead cells and cells outside of the microgel sphere are observed because of the extra time taken during the experimentation process to troubleshoot the flow through the device.

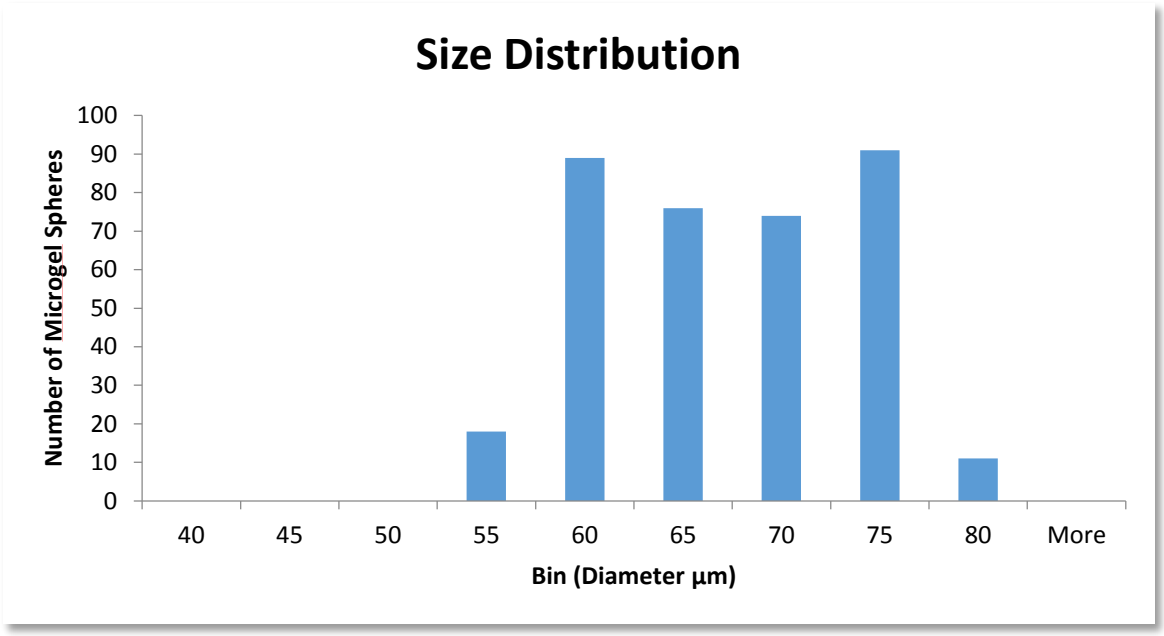

Fig. 6. Size distribution of microgel spheres.

Size distribution of the microgel spheres showed that the average sphere diameter was 64.9 ± 6.4 µm, which was within the desired sphere size of 50-70 µm.

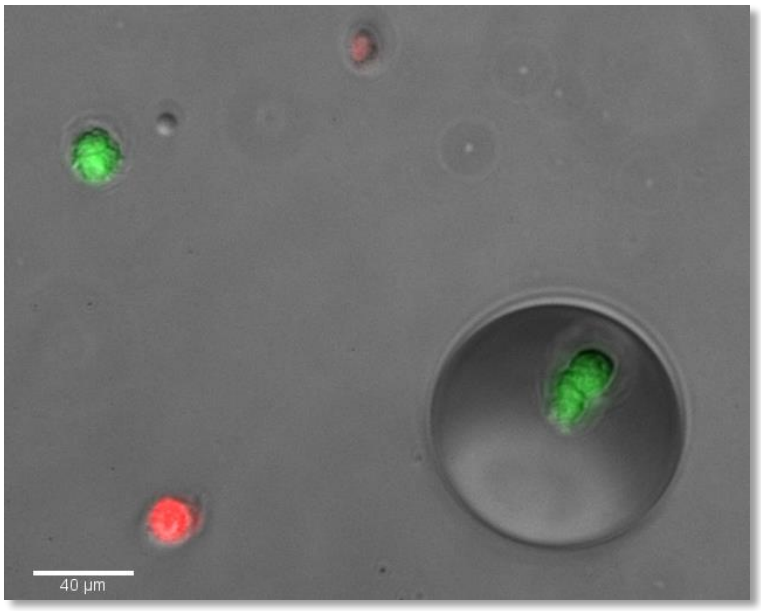

Fig. 7. U87MG cells, cell encapsulation in a microsphere.

Chapter 5 – Final Design and Verification

The serpentine design exposed the microgel spheres to the ultraviolet light for a longer time period than the straight channel inducing photocrosslinking. The serpentine design for the microfluidic device was chosen over the straight channel design because it allowed for more fully crosslinked microgel spheres. Our microfluidic design did not include a collection chamber in order to prevent coalescence of the microgel spheres within the chamber. Also a collection chamber was not included to allow for easier transport of the microgel spheres out of the device. A flow-focusing junction was chosen for our final design over a T-junction because the flow-focusing design has been seen to form monodisperse microgel spheres more consistently than the T-junction.

Originally the two solutions flowing into the two inlets of the device contained Irgacure, hyaluronic acid, and cells in one solution with the mineral oil and surfactant in the other. This was improved by moving the Irgacure into the mineral oil and surfactant solution in order to reduce

cell toxicity. The final solution of the Irgacure, mineral oil, and surfactant solution contained mineral oil, 0.5% Irgacure, 5% Span 80, and 0.05% solvent blue. The final solution for the hyaluronic acid and cells contained 0.75% HA and cells. Flow rates were determined for each of the solutions through hyaluronic acid in order to attain microgel spheres with a diameter of the desired size range between 50-70µm. The flow rate determined for the Hyaluronic acid and cells solution was 50 µl/hr and the flow rate determined for the surfactant, Irgacure, and mineral oil solution was 250 µl/hr.

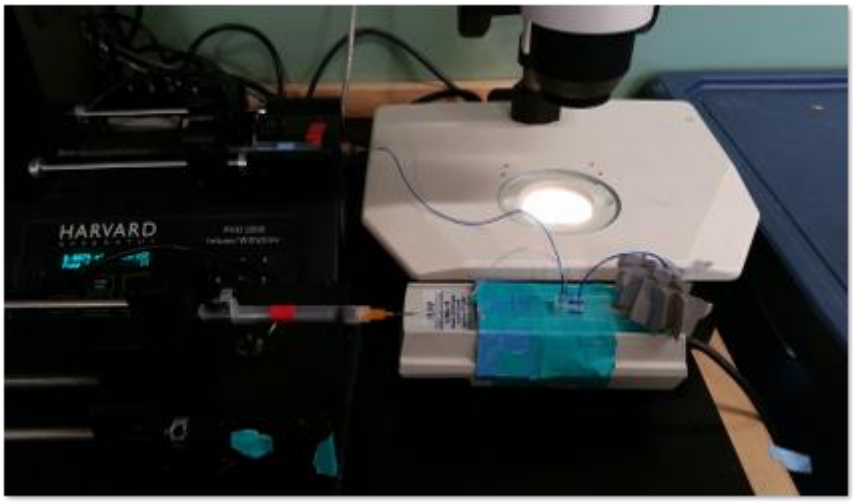

Fig. 8. Experimental Set-up

Chapter 6 – Discussion

6.1 – Gelation Testing

The first test completed for this project was an attempt at achieving hydrogel gelation within a 24 well plate. The goal behind this test was to observe gelation of the hydrogel at a visible scale outside of the device. These tests were done to ensure that the device would not be run for a long period of time, only to learn that the hydrogel didn't form all along. The belief was that the effect of the plate would be negligible on UV blocking, as would the glass plate used for the device.

Much of the initial period was spent experimenting with different ratios of hyaluronic acid and irgacure. Different ratios of 0.75% HA and 0.5% w/v irgacure were tested to determine which mixture delivered the best gelation results. Experiments that increased the amount of both the irgacure and HA in the solution resulted in no gelation through December 2nd.

The other factor that was considered was total volume in the well plate, specifically, the height of the gel in the plate that was exposed to UV. The more gel solution in the plate at a time, the more difficult it will be to cause the solution to form into a hydrogel. As seen in Chapter 5, most of the microgel spheres formed in the device had a diameter of ~70 μm. Since the diameter of the well plate was 6.5 mm, a height of 70 μm would be achieved in the 24 well plate by inserting a volume of just 2.32 μL. Smaller amounts of the solution were used in the well plate as the tests proceeded.

In the end, it was determined that the core of the issue was the procedure used to prepare the hydrogel. The steps necessary to prepare hyaluronic acid hydrogel are very exact, and must be followed precisely. Deviations in the pH and procedure time can sabotage a batch of hyaluronic acid. Once the process for HA formation was refined, gelation results improved significantly.

Hydrogel formation was achieved using a combined HA/irgacure solution a 20 μL. Since this volume was significantly larger than the microgel spheres, the experimental process could move forward.

6.2 – Microgel Sphere Formation

Optimization of the microgel sphere formation process was another major task. Many issues can arise during this process that had to be accounted for. Many flow rates will not allow for microgel sphere formation in the device. The HA may flow out of the device in a stream, or in some cases the HA will be pushed back into the syringe by the oil flow. In addition, coalescence of the microgel spheres within the device is a major issue that can disrupt their formation. This issue led to the removal of the collection chamber from the device, since this is where much of the coalescence occurred. One side effect of the ultraviolet crosslinker is hydrogel formation at the inlet, which blocks the flow of microgel spheres through the device. When all of these issues were prevented, testing can focus on optimizing the size consistency of the microgel spheres.

Determining the flow rate for the device inlet is a balancing act between a desire for efficiency and the need for stability. Running the device too fast can cause issues with microgel sphere formation at the inlet, and increases the risk of coalescence in the outlet tubing. However, the device is able to form consistent microgel spheres at a rapid rate when operated correctly. Good microgel sphere formation occurred by running the HA at 50 μL/hr and the oil at 250 μL/hr. It was observed that microgel sphere size is determined by the ratio of HA rate to oil rate. The higher the oil rate was compared to the HA rate, the smaller the microgel spheres were.

Another issue that occurred in the process was gelation at the inlet. It was initially believed this to be the result of the ultraviolet light causing crosslinking at the inlet of the device. To account

for this, the UV light was focused on the outlet of the tubing, directing it away from the inlet. Gelation at the inlet still occurred even with this change. This problem was eventually solved by altering the location of the irgacure. Initially, the irgacure was mixed in with the HA, and oil was ran on the other side. Putting the irgacure in with the oil instead of the HA remedied the problem.

The device was able to generate consistent microgel spheres within the range of 55-80 μm diameter. Size consistency was important for the reliability and therapeutic efficiency of the device. To verify this, a high speed camera was used to capture the microgel formation process, and measured the diameter of the microgel spheres. A list of the data received from this test is available in Appendix B.

6.3 – Cell Encapsulation

Arguably the most important element of this project was the success in encapsulating cells. In order to measure cell encapsulation, a new system of imaging had to be developed. This method involved staining the cells with two chemicals, calcine, and ethidium homodimer. Calcine is a green stain, and is able to detect the presence of live cells in the solution. Ethidium homodimer is a red stain, capable of detecting the presence of dead cells in the solution. By using a fluorescence microscope, the solution could be imaged to observe for the presence of cells. These images would then be superimposed onto an image of the microgel spheres themselves, taken under a regular microscope. If the cells matched up with the microgel sphere boundaries, it was assumed that encapsulation was successful.

The experiment on March 3rd was the most effective experimental run for cell encapsulation, both devices produced clearly visible cell encapsulation. U87 cells were encapsulated, with visualization of the encapsulation available in the image in the results section

of the paper (Chapter 5). For these, the oil was stained to help us discern where the cells wound up in the solution to ease the imaging process.

For the March 17th and March 24th experiments, microgel sphere formation and gelation was observed but no encapsulated cells were found during encapsulation. It is possible that the cells were not adequately mixed into the HA solution. Cells could have sank to the bottom of the tube, and the experiment could have been stopped before the cells with the HA were flowed through the device.

6.4 – Economic and Social Implications

Economically, the project should not drastically increase the cost of spinal therapy. Compared to the cost of spinal cord therapy, the materials needed for this project are relatively inexpensive. Nevertheless, adding another element to the therapy would marginally increase the cost of the procedure. Materials and equipment would need to be purchased, and additional time would need to be spent running the equipment. The crucial question then for anyone attempting to incorporate this therapy into the surgical procedure, is whether or not the benefits of the project outweigh the additional cost. If this project can take a surgery that was previously impossible due to cell survival issues, and turn it into a feasible treatment, then the cost of the procedure would be justified.

The project should have a low environmental risk factor attached to it. None of the chemicals used in the process are released into the environment because the process is ran in a controlled laboratory setting. The biggest environmental risk of the project to be controlled is biological waste disposal. The experimental procedure requires the disposal of unused cells, as well as media, hyaluronic acid, and oil, among other products. For this, it is crucial that the

laboratory running these procedures uses proper biohazard waste procedures to avoid chemicals from the lab entering the environment.

This project is not a therapy in of itself, rather the process developed will be used in hospitals to develop materials used in spinal cord therapy. Commercialization of this project would likely occur through a private company, which would develop the equipment to be sold directly to hospitals for their use in surgical procedures. Patients would not likely see these sales firsthand, as they are usually done between businesses. However, the need to incorporate more equipment into the procedure would likely increase the cost of the procedure.

As with most new medical technologies, this product would likely be more available in first-world countries such as the United States, Japan, and Western Europe, where hospitals can afford these devices. If the product can be used to make stem cell CNS therapy a more viable procedure, then stem cell CNS therapy would then become even more available in these developed countries than in other less developed countries.

This project would improve the lives of patients with CNS trauma by improving the quality of the surgery they can receive. Since currently only 5-10% of implanted neural stem cells survive in current stem cell therapies, this project would make treatments that were previously unfeasible available for use. For the patients who would receive these surgeries, this project would of great benefit. However, this project could also pose health risks to patients. The biggest danger the team worries about in this is the risk of viral infection through the cells. In many cases, this could put the patient at risk of death. This risk however, is consistent with any type of cell based therapy, regardless of encapsulation. From this perspective, this project poses no additional risk to the patient.

Manufacturing of this project will likely be the single greatest challenge that any team faces in the development of this project for commercial use. The device designed through this project is capable of producing about 50 µl of microgel spheres an hour. This is just a prototype, and will need to be scaled up to produce enough microgel spheres to be useful in therapy. One possible solution would be to create a device that uses many PDMS devices to create enough microgel spheres for usage in therapy.

Chapter 7 – Conclusions and Recommendations

At the conclusion of this project, a flow focus serpentine microfluidic device capable of producing microgel spheres within the desired size range (50-70µm diameter) was modified and developed. In addition, a protocol for cell encapsulation was refined through experimentation. This protocol includes the system set-up, device dimensions, flow rates, inlet solution concentrations and volumes, and number of cells. The successful encapsulation of U87MG cells into microgel spheres is proof of concept for future experimentation in applying microfluidics for transplanting viable NSCs, which has not yet been attempted. This microfluidic system shows promise for successful and high throughput cell encapsulation, but needs to be further developed before use as a cell therapy delivery mechanism.

There are several recommendations to improve the process and increase success. First and foremost, the team recommends changing the angle in the device to allow for better flow and reduce clogging in the device. Throughout the project, the team encountered several setbacks due to device clogging. Experimentation with the different angles within the device may lead to a decrease in troubleshooting time and overall process time, which would increase cell viability.

A minor but potentially beneficial recommendation is to use a UV light source with a smaller diameter. The team noticed occasional inlet clogging due to premature hydrogel crosslinking. The current set-up utilized a UV source that was wider than the desired region for crosslinking. Using a UV light source with a smaller diameter would decrease inlet clogging and allow for more control of light placement on the crosslinking channel. With decreased inlet clogging, the overall process time would decrease.

The team also recommends expanding the imaging protocol. The microgel spheres can be difficult to image for several reasons. First, the microgel spheres lose their shape when imaged with glass slides and covers slips and are not stationary when imaged in well plates. In addition, a dimension of the spheres is lost with two-dimensional imaging systems. Bright field and fluorescence imaging serve as sufficient methods for determining if cells were encapsulated but don't provide the exact placement of the cells within the microgel sphere. A layer by layer imaging approach could be used to better understand the placement of cells within the microgel spheres.

Before this system can be used to encapsulate cells for in vitro or in vivo use, the team recommends creating a storage system and incorporating biomarkers. While the exact set-up and parameters of the storage system are undefined, it would have to maintain the microgel spheres integrity and cell viability. One of the main issues associated with NSC therapy is that only 5-10% survive host immune response and inflammation. Biomarkers and bioactive molecules should be incorporated into the hydrogel to increase cell viability. In particular, the Fas ligand can be attached to the hydrogel backbone through the thiol groups. The Fas ligand can bind to immune cells and induce apoptosis, thereby increasing cell viability.

A microfluidic system was created to encapsulate cells in to microgel spheres. Although this system and corresponding protocols require further optimization and experimentation, it shows promise. Once optimized, this system can be applied not only to encapsulating NSCs for neurological cell therapy, but also to other cell types. This technology has the potential to revolutionize current stem cell therapy practices.

References

Aarli, J., Dua, T., Janca, A., & Muscetta, A. (2006). Neurological disorders public health challenges. Geneva: World Health Organization. Retrieved from: http://www.who.int/mental_health/neurology/neurodiso/en/

Albrecht, D. (2014). Microfluidic Physics I: Flow, Resistance, Diffusion, (and Droplets?). Worcester Polytechnic Institute.

Banerjee, A., Arha, M., Choudhary, S., Ashton, R. S., Bhatia, S. R., Schaffer, D. V., & Kane, R. S. (2009). The influence of hydrogel modulus on the proliferation and differentiation of encapsulated neural stem cells. *Biomaterials, 30*(27), 4695-4699. doi: http://dx.doi.org/10.1016/j.biomaterials.2009.05.050

Baret, J.-C. (2012). Surfactants in Droplet-Based Microfluidics. Lab on a Chip.

Baruch, L., & Machluf, M. (2006). Alginate–chitosan complex coacervation for cell encapsulation: Effect on mechanical properties and on long-term viability (Vol. 82, pp. 570-579). Biopolymers.

Bransky, A., Korin, N., Khoury, M., & Levenberg, S. (2009). A microfluidic droplet generator based on a piezoelectric actuator. *Lab on a Chip, 9*(4), 516-520. doi: 10.1039/B814810D

Casquillas, G., (2015). *Introduction to polydimethylsiloxane (PDMS)*. Retrieved January, 2015, from http://www.elveflow.com/microfluidic- reviews-and-tutorials/the-poly-di-methyl-siloxane-pdms-and-microfluidics

Ehtesham, M., Kabos, P., Kabosova, A., Neuman, T., Black, K. L., & Yu, J. S. (2002). The Use of Interleukin 12-secreting Neural Stem Cells for the Treatment of Intracranial Glioma.

Fahn, S., Oakes, D., Shoulson, I., Kieburtz, K., Rudolph, A., Lang, A., . . . Parkinson Study, G. (2004). Levodopa and the progression of Parkinson's disease. *The New England journal of medicine, 351*(24), 2498-2508. doi: 10.1056/nejmoa033447

ffrench, C. (2008). The neural stem cell microenvironment. *Stem book*.

Flow control in microfluidic devices. (n.d.). Retrieved April 26, 2015, from http://www.elveflow.com/microfluidic-reviews-and-tutorials/flow-control-in-microfluidic-device

Gregory, M. S., Repp, A. C., Holhbaum, A. M., Saff, R. R., Marshak-Rothstein, A., & Ksander, B. R. (2002). Membrane Fas Ligand Activates Innate Immunity and Terminates Ocular Immune Privilege. *The Journal of Immunology, 169*(5), 2727-2735.

Griffith, T. S., Brunner, T., Fletcher, S. M., Green, D. R., & Ferguson, T. A. (1995). Fas Ligand-Induced Apoptosis as a Mechanism of Immune Privilege. *Science, 270*(5239), 1189-1192. doi: 10.1126/science.270.5239.1189

Hager, D. B., & Dovichi, N. J. (1994). Behavior of Microscopic Liquid Droplets near A Strong Electrostatic Field: Droplet Electrospray. *Analytical Chemistry, 66*(9), 1593-1594. doi: 10.1021/ac00081a040

Hayworth, D. (2014). Chemistry of Crosslinking: Thermo Fisher Scientific Inc.

Hunt, N., & Grover, L. (2010). Cell encapsulation using biopolymer gels for regenerative medicine. *Biotechnology Letters, 32*(6), 733-742. doi: 10.1007/s10529-010-0221-0

Ifa, D. R., Wu, C., Ouyang, Z., & Cooks, R. G. (2010). Desorption electrospray ionization and other ambient ionization methods: current progress and preview. *Analyst, 135*(4), 669-681. doi: 10.1039/B925257F

Jayasinghe, S. N. (2011). Bio-electrosprays: from bio-analytics to a generic tool for the health sciences. *Analyst, 136*(5), 878-890. doi: 10.1039/C0AN00830C

Jayasinghe, S. N., Qureshi, A. N., & Eagles, P. A. M. (2006). Electrohydrodynamic Jet Processing: An Advanced Electric-Field-Driven Jetting Phenomenon for Processing Living Cells. *Small, 2*(2), 216-219. doi: 10.1002/smll.200500291

Kazanis, I., Lathia, J., Moss, L., and ffrench-Constant, C., The neural stem cell microenvironment (August 31, 2008), StemBook, ed. The Stem Cell Research Community, StemBook, doi/10.3824/stembook.1.15.1, from http://www.stembook.org.

Kennea, N. L., Weston Laboratory, I. o. R. a. D. B., Division of Paediatrics, Obstetrics and Gynaecology, Imperial College of Science, Technology and Medicine, London W12 0NN, UK, Mehmet, H., Weston Laboratory, I. o. R. a. D. B., Division of Paediatrics, Obstetrics and Gynaecology, Imperial College of Science, Technology and Medicine, London W12 0NN, UK, & Weston Laboratory, I. o. R. a. D. B., Division of Paediatrics, Obstetrics and Gynaecology, Imperial College of Science, Technology and Medicine, Hammersmith Hospital Campus, Du Cane Road, London W12 0NN, UK. (2014). Neural stem cells. *The Journal of Pathology, 197*(4), 536-550. doi: 10.1002/path.1189

Li, J. H., Department of Immunology Weizmann Institute of Science, R., Israel, Rosen, D., Department of Immunology Weizmann Institute of Science, R., Israel, Sondel, P., Departments of Pediatrics, H. O. a. G., University of Wisconsin Comprehensive Cancer Center, Madison WI, USA, . . . Department of Immunology Weizmann Institute of Science, R., Israel. (2014). Immune privilege and FasL: two ways to inactivate effector cytotoxic T lymphocytes by FasL-expressing cells. *Immunology, 105*(3), 267-277. doi: 10.1046/j.1365-2567.2002.01380.x

Lindvall, O., & Kokaia, Z. (2006). Stem cells for the treatment of neurological disorders. *Nature, 441*(7097), 1094-1096.

Madigan, N., McMahon, S., O'Brien, T., Yaszemski, M., & Windebank, A. (2009). Current Tissue Engineering And Novel Therapeutic Approaches To Axonal Regeneration Following Spinal Cord Injury Using Polymer Scaffolds. *Respiratory Physiology & Neurobiology, 169*(2), 183-199. doi:doi:10.1016/j.resp.2009.08.015

Medicine, U. S. N. L. o. (2000, 2000-01-05). Neurodegenerative Diseases. Retrieved September, 2014, from http://www.ncbi.nlm.nih.gov/pubmed/

Mongkoldhumrongkul, N., Swain, S. C., Jayasinghe, S. N., & Stürzenbaum, S. (2009). Bio-electrospraying the nematode Caenorhabditis elegans: studying whole-genome transcriptional responses and key life cycle parameters. *Journal of The Royal Society Interface*.

Nguyen, K. T., & West, J. L. (2002). Photopolymerizable hydrogels for tissue engineering applications. *Biomaterials, 23*(22), 4307-4314. doi: http://dx.doi.org/10.1016/S0142-9612(02)00175-8

Nicodemus, G., & Bryant, S. (2008). Cell Encapsulation in Biodegradable Hydrogels for Tissue Engineering Applications (pp. 149-165). University of Colorado: Mary Ann Liebert, Inc.

PDMS: A review. (n.d.). Retrieved April 26, 2015, from http://www.elveflow.com/microfluidic-reviews-and-tutorials/the-poly-di-methyl-siloxane-pdms-and-microfluidics

Piotr, G., Michael, F., Howard, S., & George, W. (2006). Formation of droplets and bubbles in a microfluidic T-junction—scaling and mechanism of break-up. doi: 10.1039/B510841A

Purves, D., Augustine, G. J., Fitzpatrick, D., Katz, L. C., LaMantia, A.-S., McNamara, J. O., & Williams, S. M. (2001). Neuroglial Cells. doi: http://www.ncbi.nlm.nih.gov/books/NBK10869/

Risbud, M., Endres, M., Ringe, J., Bhonde, R., & Sittinger, M. (2001). Biocompatible hydrogel supports the growth of respiratory epithelial cells: Possibilities in tracheal tissue engineering (Vol. 56, pp. 120-127). Biomedical Materials.

Saha, K., Keung, A. J., Irwin, E. F., Li, Y., Little, L., Schaffer, D. V., & Healy, K. E. (2008). Substrate Modulus Directs Neural Stem Cell Behavior. *Biophysical Journal, 95*(9), 4426-4438. doi: http://dx.doi.org/10.1529/biophysj.108.132217

Sayegh, M. H., & Turka, L. A. (1998). The role of T-cell costimulatory activation pathways in transplant rejection. *The New England journal of medicine, 338*(25), 1813-1821.

Stille, J. K. (1981). Step-Growth Polymerization. doi: 10.1021/ed058p862

The role of feedback in microfluidic flow-focusing devices. (n.d.). Retrieved April 26, 2015, from http://rsta.royalsocietypublishing.org/content/366/1873/2131

The National Spinal Cord Injury Statistical Center. (2011). Spinal Cord Injury Facts and Figures at a Glance. *Journal of Spinal Cord Medicine, 34*(6), 620-621. doi:10.1179/204577211X13218754005537

Teh, S.-Y. (2008). Droplet Microfluidics. In R. H. Lin (Ed.). Lab on a Chip.

WebMD, L. (2014). Glossary of Alzheimer's Disease Terms. Retrieved September, 2014, from http://www.webmd.com/alzheimers/glossary-terms-alzheimers?page=6

Workman, V. L., Tezera, L. B., Elkington, P. T., & Jayasinghe, S. N. (2014). Controlled Generation of Microspheres Incorporating Extracellular Matrix Fibrils for Three-Dimensional Cell Culture. *Advanced Functional Materials, 24*(18), 2648-2657. doi: 10.1002/adfm.201303891

Yang, J.-A., Yeom, J., Hwang, B. W., Hoffman, A. S., & Hahn, S. K. (2014). In situ-forming injectable hydrogels for regenerative medicine. *Progress in Polymer Science*(0). doi: http://dx.doi.org/10.1016/j.progpolymsci.2014.07.006

Youdim, M. B. H., & Buccafusco, J. J. (2005). Multi-functional drugs for various CNS targets in the treatment of neurodegenerative disorders. *Trends in Pharmacological Sciences, 26*(1), 27-35. doi: http://dx.doi.org/10.1016/j.tips.2004.11.007

Young, C. J., Poole-Warren, L. A., & Martens, P. J. (2012). Combining submerged electrospray and UV photopolymerization for production of synthetic hydrogel microspheres for cell encapsulation. *Biotechnology and Bioengineering, 109*(6), 1561-1570. doi: 10.1002/bit.24430

Appendix A: Experimental Protocols

Silicon Master Formation (Soft Lithography)

1. Dehydration Bake
    a. Turn on the blower and light on the hood. Let it run for a few minutes before working inside.
    b. Power on the hot plate in the clean hood. Ensure the hotplate surface is clean.
    c. Set the temperature to 120 °C.
    d. Place a clean new wafer onto the hotplate surface. The whole wafer should completely fit on the hotplate surface so that heat can conduct evenly to the wafer.
    e. Once the plate reaches the desired temperature, heat for 5 min.
    f. Carefully remove from the hotplate with wafer tweezers and allow to cool to room temperature. The wafer is now ready for the next procedure.
2. Spin-coating
    a. Turn on the two 7" hotplates.
    b. Set the left one to 65 °C and the right one to 95 °C.
    c. Set the spin program according to the description below
        i. The first step is a slow ramp to 500 rpm at 100 rpm/s and is designed to slowly spread the resist across the wafer. The second step spins faster to determine the final resist film thickness. Change the spin speed to account for different resist thickness
    d. Remove the spin-coater lid and verify the presence of a foil liner. If the foil is not present, line the bowl with foil to catch photoresist that is removed from the wafer during spinning. Ensure that the bowl periphery is covered above the height of the chuck and wafer, and also completely covering the bottom to the chuck. Rotate the chuck and ensure that the foil does not touch the chuck or impede rotation.
    e. Turn on the nitrogen supply, by opening the main tank valve. Ensure an output pressure of 60-70 psi.
    f. Make sure that the wafer is clean and dry. Visible dust on the wafer can be removed by gently blowing the wafer using the nitrogen gun.
    g. Position the 4" wafer alignment tool against the chuck, and place the wafer on the chuck aligning to the marks on the alignment tool.
    h. Before removing the alignment tool, turn on the vacuum. The wafer should now be held down on the chuck.
    i. Test your alignment by beginning the spin program. The wafer should wobble less than 5 mm.
    j. Ensure the wafer is centered and the spin-coater is programmed and ready to spin.

k. Pour approximately 8-10 mL of resist onto the wafer in one continuous motion, with the tube far enough to avoid contact with the wafer but close enough to prevent thin filaments of resist from forming: about 1 cm. Once the resist blob covers about 5cm diameter, quickly move the tube toward the edge while tilting the tube upwards and twisting to prevent drips on the outside of the tube.
l. Start spin coating. The spin coating process takes about 1 minute. The spinner will stop automatically when spin coating is completed.
m. Verify that the photoresist has been uniformly coated. If striations and streaks are observed, the spin coating was not successful. Some causes may include:
    i. dust particles on the surface (clean it better),
    ii. bubbles in the photoresist (heat the resist tube to 40-50 °C in a water bath to remove them; see resist datasheet for more information)
    iii. insufficient resist volume applied
n. Release the chuck vacuum.

3. Prebake (Soft Bake)
    a. Transfer the wafer from the spinner chuck to the 65 °C hotplate. Set the timer to 3 minutes and cover the wafer with a foil tent.
    b. Transfer the wafer from the 65 °C hotplate to the 95 °C hotplate. Set the timer to 9 minutes and cover the wafer with a foil tent
    c. Return the wafer to the 65 °C hotplate for 3 minutes, covered, then transfer it to the clean hood to cool to room temperature.
4. UV exposure
    a. Turn on the UV exposure unit.
    b. Unlock the drawer of the UV exposure unit. If there is a wafer or mask present, remove them. Place the 4"x 5" glass slide on the tray and wave near the door sensor to close it.
    c. Calibrate the UV intensity. It should display about 23.4 mW/cm2 through the glass plate.
    d. Program the desired exposure duration and intensity, in our case 14 s.

$$\frac{230\,\frac{mJ}{cm^2}\ x\ 1.5}{23.4\,\frac{mW}{cm^2}} = Exposure\ Time\ (s)$$

    e. Start the exposure. Verify that the countdown timer begins at the proper duration.
    f. The exposure will end automatically and alert with a loud beep. Remove the glass slide if present.
    g. Transfer the room temperature, resist-coated wafer to the UVKUB tray, centering it in the circular pattern.

h. Observe the position of any defects in the resist layer. Try to rotate your photomask such that these defects are removed during development.
i. Cut out the photomask circle using scissors. Ensure it is free of dust, and gently wipe with a lint-free cleanroom wipe or blow with the nitrogen gun if necessary.
j. Place the photomask over the resist-coated wafer and orient it such that any defects will be removed during development.
k. Place the 4" x 5" glass slide over the wafer and mask to keep it flat and in direct contact. When you are satisfied with the mask orientation and glass plate placement, close the door.
l. Run the previous exposure program. Verify the correct exposure intensity
m. The exposure will end automatically and alert with a loud beep. The drawer opens automatically.
n. Gently lift the glass slide with wafer tweezers and set aside. Gently lift the photomask with wafer tweezers and set aside.
o. Observe the resist surface. At this point, no pattern should be easily visible. If it is, the exposure time was too long.

5. Post-Exposure Bake (PEB)
    a. Transfer the wafer from the UV exposure unit to the 65 °C hotplate in the fume hood. Be sure to place your hand underneath as you move the wafer so it doesn't drop. Set the timer for the desired time at this PEB temperature (3 minutes).
    b. Observe the resist surface. With ideal exposure, the mask pattern will become slightly visible in 5-30 s. Cover with a foil tent.
    c. Transfer the wafer from the 65 °C hotplate to the 95 °C hotplate and cover. Set the timer for the desired time at this temperature (9 minutes).
    d. Return the wafer to the 65 °C hotplate for 3 minutes, then transfer it to a cleanroom wipe on the work surface to cool to room temperature. At this point, the mask pattern should be clearly visible. If not, exposure and/or baking times were too short.
6. Development
    a. Ensure the glass dish is clean, clean if necessary. Pour developer in the dish to about 0.5-1 cm depth.
    b. Immerse the wafer in developer and gently slosh/agitate, taking care not to splash developer out of the dish. Set a timer for 7-10 minutes.
    c. Observe the wafer periodically. Bare Si regions will become visible after ~30s - 1 min. The resist at the edge is thicker than in the center, and therefore tends to be the last part to dissolve away.
    d. When all resist appears dissolved, remove it from the developer bath with wafer tweezers and run under a gentle stream of water in the hood sink.

   e. After both front and back sides are rinsed in water, dry both sides with the nitrogen gun.
   f. Inspect the wafer for any cracks or other issues. Perform a final cleaning development by holding the wafer with tweezers horizontally over the dish and squirting a small amount of fresh developer on the wafer. Gently slosh side-to-side for about 15s. Rinse with water and dry with a nitrogen gun.
7. Post-bake
   a. Place the developed wafer on a hotplate at no more than 65 °C.
   b. Set the ramp rate to 6 °C/min or 360 °C/hr. Set temperature to 150°C. Set the timer for 45 minutes. Set the hotplate to automatically turn off then the timer ends. Cover with a foil tent.
   c. The hotplate will slowly ramp up to 150°C over about 15 minutes, maintain temperature for ~30mins, then turn off and slowly return to room temperature. This will take around 1 hr total.
   d. After the wafer has returned to room temperature, inspect the wafer again and verify that surface cracks have disappeared. Document selected microscope fields with a camera.

PDMS Device Formation

1. Create a 10:1 mixture of PDMS, using 50 g of the PDMS base, and 5 g of the PDMS curing agent
2. Stir the mixture for 5-10 minutes, being sure to mix the edges in addition to the center. Make sure the full solution is mixed by lifting PDMS from the bottom to the top
3. Place the PDMS mixture into the vacuum chamber for 45 minutes, to remove any air bubbles.
4. Pour the PDMS mixture into the device mold. If any air bubbles are present, move them away from the device
5. Leave the device mold in the oven at 65 °C overnight, for at least twelve hours.
6. Remove the device mold from the oven.
7. Use a razor blade to cut the devices out of the PDMS mold.
8. Punch holes through the inlets and outlets of the device. This can be done efficiently using these steps.
   a. Place a piece of scotch tape on the side of the device with the engravings
   b. Use a sharpie to draw in the locations of the inlets and outlets onto the tape
   c. Use a holepuncher to pierce into the inlets through the tape side going all the way through the device. Remove the scrap from the holepuncher before removing
9. Plasma bond the PDMS device to the glass slide. This can be done effectively using these steps.

   a. Place the PDMS device onto the base slide with the engravings facing up.
   b. Place the glass slide to be used onto the base slide next to the PDMS
   c. Insert the base slide into the plasma bonder. Close the door and form the vacuum seal
   d. Turn the plasma bonder on. Expose the materials to the plasma for 30 seconds
   e. Remove the materials from the plasma bonder. As quickly as possible place the PDMS engraving side against upward facing side of the glass slide
   f. Hold the PDMS against the glass slide for at least two minutes. Make sure the entire PDMS is connected to the glass slide
10. Place the PDMS device into the oven at 80 °C for 48 hours.
11. Once the PDMS is removed from the oven, it is ready to be used.

Hyaluronic Acid Formation

1. Prepare 1% w/v solution of high MW HA
   a. Dissolve 0.25 g of high MW HA in 25mL 0.01M NaOH solution with a pH of 12.5
   b. Place pure HA mixture on rotisserie shaker in room temperature overnight or for 4 hours for complete dissolution
2. Acrylate HA polymer with divinyl sulfone (DVS)
   a. Add 597 µl of DVS
   b. React mixture under continuous vortexing for 5 minutes and on the rotator for 15 minutes, protected from light by aluminum foil
   c. The solution should be at pH 12
3. After 20 minutes, quench the reaction with 1.5M HCl
   a. The volume of HCl added will depend on the initial pH of the solution. After quenching, the solution should be at pH 5 (pH 5.0-5.2)
   b. Note: About 150-300 µl may be added. Add in slowly and consistently check pH
4. Dialyze with 25k dialysis bags against diH_2O in the cold room
   a. Change water bath every 4 hours to remove excess DVS and allow dialysis to occur in clean water
5. After 48 hours, separate 25 mL mixture into 3 separate opaque 50 mL conical tubes. Seal with parafilm, and store in -80 °C to freeze. Sample must be frozen prior to lyophilization
6. After 48 hours, the solution must be lyophilized
   a. Start the lyophilizer, and wait 30 minutes for equalization
   b. During equalization, seal tubes with frozen HA using kimwipes and rubber band. Place in jar and lyophilize
   c. When finished, place the lyophilized HA samples in the freezer in the dessicater, protected from light.

Hyaluronic Acid Reconstitution

1. Dissolve acrylated HA in PBS
    a. Pour 10 mL of PBS into a 15 mL conical tube
    b. Add 0.075 g acrylated HA into the PBS solution
    c. Vortex the solution until all of the acrylated HA is dissolved

$$Mass\ (g) = \frac{\frac{w}{v}\%}{100}\ X\ volume\ (mL)$$

$$Mass = \frac{0.75\ wt\%}{100}\ X\ 10 = 0.075\ g$$

Oil, Surfactant, Irgacure and Dye Formation

1. Add 10 mL of mineral oil to a 15 mL conical tube
2. Add 0.5 mL of surfactant to the solution (5% oil volume)
3. Add 0.05 g of Irgacure 2959 to the solution (0.5% oil volume)
4. Add 0.005 g of solvent blue to the solution (0.05% oil volume)

Cell Culture

1. Perform trypsinization, (if necessary)
2. Pipette cell culture into a 15 mL conical tube
3. Spin down in centrifuge
4. Resuspend cell culture in media
5. Count the cells using the hemacytometer
    a. Insert 10 µl of the cell suspension into the hemacytometer
    b. Count the total cells in the upper two, middle, and lower two grids on the hemacytometer

$$\frac{\#\ cells}{5\ boxes}\ x\ dilution\ factor\ x\ 10{,}000 = total\ cells/mL$$

6. Spin the cells in the centrifuge for 5 minutes
7. Resuspend the cells in a 1 mL of media
8. Aliquot 1 mL of reconstituted HA into the test tube
9. Add the cells to the HA solution
10. Resuspend the cells using the pipet aid
11. Vortex the solution for 30 seconds
12. Pour cell solution into the syringe
13. Make sure no bubbles are present in the tube

Apparatus Setup

1. Place PDMS device under a microscope attached to a computer with imaging software
2. Add the cell/HA solution to syringe #1
3. Add the oil mixture to syringe #2
4. Place tubing into an aliquot tube containing cell media, and connect the other end of the tube to the device outlet
5. Connect the syringe tubing to the respective inlets on the PDMS device

Microfluidic Device Operation

1. Prior to the experiment
    a. Set diameter to 8.76 mm
    b. Set syringe #1 flowrate to 50 µl/hr
    c. Set syringe #2 flowrate to 250 µl/hr
2. Start both syringes at the same time
3. Wait until droplets are forming inside of the device
    a. If droplets are not forming after 10 minutes, increase both flow rates and then decrease to the specified values in step 1
4. Once droplets are being formed, move device from the microscope to the UV light.
5. Collect the droplets in the media within tube
6. Proceed with this for 45 minutes

Droplet Imaging

1. Stain the droplets using the following steps
    a. Spin down in centrifuge for 2min. at 1000rpm
    b. Aspirate the top layer of media and oil
    c. Perform live/dead staining using the appropriate amount of stain
2. Place cells under microscope to collect fluorescent, brightfield and the overlay of the fluorescent and brightfield images

Appendix B: Size Distribution Raw Data

Microgel spheres formation was recorded using a camera

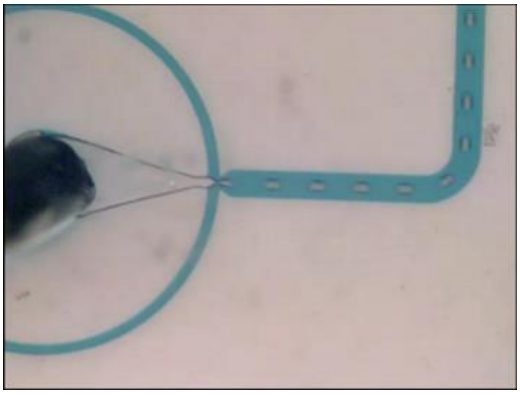

Fig. 9. Microgel spheres being formed

Microgel sphere diameters were measured using ImageJ.

Droplet	Area	Mean	Min	Max	Diameter (µm)	Average Diameter (µm)	Diameter Median (µm)	STDEV
1	155.204	127.516	122	130.333	52	64.9295766	64.119	6.407603
2	186.245	124.937	116.333	129.309	63.252			
3	170.724	126.376	115.111	130.333	59.429			
4	170.724	125.938	117.407	130	59.429			
5	162.964	126.606	113.333	130.88	54.841			
6	178.485	118.672	108.333	124.853	62.263			
7	170.724	120.129	103	129.496	59.429			
8	170.724	116.456	99.566	124.566	59.429			
9	186.245	118.348	102.556	124.984	63.143			
10	194.005	134.947	122.111	139.889	66.857			
11	170.724	139.468	128.815	145.086	59.429			
12	170.724	140.824	130.444	145.46	59.429			
13	170.724	138.437	123.889	145.81	59.429			
14	162.964	137.362	129.222	143.889	54.841			
15	201.765	130.89	111.778	141.932	69.389			
16	186.245	126.155	110.704	132.089	63.143			
17	170.724	124.546	111.63	130.464	59.429			
18	194.005	122.324	111	129.667	66.857			
19	194.005	129.301	119.778	132.815	66.857			
20	217.286	128.786	118.593	134.667	74.286			

21	225.046	128.94	116.889	135.481	78			
22	194.005	128.582	118.778	132.889	66.857			
23	170.724	128.514	124.267	136.896	58.728			
24	155.204	125.834	117.889	130.064	54.081			
25	155.204	126.574	107.444	135.135	52			
26	162.964	126.153	115.333	130.667	55.714			
27	162.964	120.36	106.778	125.778	55.714			
28	217.286	129.009	119.704	133.333	74.286			
29	225.046	133.701	119.889	139	78			
30	225.046	132.697	117.222	139.889	78			
31	201.765	131.865	121.222	136.016	70.571			
32	209.526	128.667	117.333	133.667	71.446			
33	162.964	127.662	121.074	132.422	55.838			
34	186.245	122.737	110.889	127.457	63.143			
35	155.204	132.58	118.667	136.667	52			
36	194.005	121.049	103	131.778	66.857			
37	201.765	134.871	122.667	141.031	70.571			
38	217.286	134.235	121.63	140.314	74.286			
39	186.245	133.792	120.333	143.667	66.857			
40	201.765	134.611	120.333	143.213	70.669			
41	162.964	131	121.111	142.24	55.714			
42	194.005	129.425	117	134.926	66.857			
43	170.724	124.285	115.963	128.086	59.429			
44	225.046	124.395	106.667	132.111	78			
45	162.964	127.354	110.889	134.667	55.714			
46	170.724	130.637	124	135.644	59.545			
47	201.765	133.028	120.333	137.84	70.571			
48	194.005	132.671	121.444	140	66.857			
49	217.286	128.682	120.185	136.237	74.286			
50	186.245	128.303	120.222	136.968	63.903			
51	186.245	127.469	115.889	131.149	63.252			
52	186.245	124.881	115	129.841	63.578			
53	155.204	126.771	114	131.222	52			
54	170.724	128.076	113.037	133.065	59.429			
55	186.245	140.895	130.296	145.628	63.143			
56	217.286	140.79	125.444	147.435	74.286			
57	162.964	141.344	132.63	144.926	55.714			
58	170.724	138.065	128.333	144.841	59.429			
59	186.245	134.483	125.333	142.793	63.252			
60	194.005	133.863	117.296	141.099	66.96			

61	186.245	131.364	114.889	138.333	63.143			
62	217.286	129.468	112.889	140.941	74.286			
63	170.724	131.086	119.519	135.709	59.429			
64	201.765	135.545	124.963	141.227	70.669			
65	170.724	140.932	126.222	146.111	59.429			
66	170.724	139.582	129.333	142.868	59.429			
67	194.005	138.351	126.333	143.444	66.857			
68	194.005	136.559	124.407	144	66.443			
69	209.526	132.812	114.444	139.201	72.118			
70	186.245	126.094	118.37	131.005	63.143			
71	186.245	126.006	111.778	134	63.143			
72	155.204	128.417	120.333	130.333	55.714			
73	194.005	143.587	130.333	149.222	66.857			
74	217.286	145.369	129.667	151.218	74.286			
75	225.046	143.318	132.889	151.556	78			
76	194.005	142.381	128.741	148.815	66.857			
77	186.245	144.68	131.012	149.82	64.119			
78	162.964	141.52	128.889	147.124	54.841			
79	217.286	134.946	118	142.736	74.379			
80	186.245	135.22	115.111	143.863	63.143			
81	170.724	131.614	118	138.102	59.429			
82	162.964	148.09	139.185	152.333	55.714			
83	201.765	147.797	132.444	153.867	70.571			
84	201.765	145.622	136.333	149.622	70.571			
85	201.765	144.61	127.556	150.853	70.669			
86	162.964	145.569	133.667	152.156	55.217			
87	170.724	143.861	128.407	149.026	59.429			
88	162.964	142.852	133	147	55.714			
89	186.245	134.493	115.63	140.929	63.143			
90	217.286	135.695	119.503	145.977	74.286			
91	194.005	140.403	122.741	146	66.857			
92	225.046	142.28	123.333	149.852	78			
93	194.005	142.404	128.333	148	66.857			
94	217.286	140.05	125.63	148.506	74.286			
95	186.245	139.867	127	147.013	64.867			
96	155.204	137.087	129.444	143.964	54.081			
97	162.964	132.869	120.111	138.778	55.838			
98	186.245	134.756	120.481	140.683	63.143			
99	170.724	125.794	112.778	134.287	59.429			
100	201.765	131.228	117.333	137	70.571			

101	186.245	133.486	125.667	137.667	66.857			
102	186.245	132.941	125	137.729	63.143			
103	170.724	134.157	122.111	138.125	59.429			
104	170.724	130.108	123.001	136.125	58.019			
105	217.286	119.393	105.136	128.505	74.286			
106	201.765	125.926	107.556	133.333	70.571			
107	186.245	127.89	108	139	63.143			
108	194.005	123.249	109.37	130.037	66.857			
109	186.245	135.423	123.074	137.965	63.143			
110	217.286	141.757	123	149.34	74.286			
111	201.765	140.996	126.667	147.333	70.571			
112	194.005	140.699	126.037	145.926	66.857			
113	217.286	137.677	118.222	146.77	74.286			
114	178.485	137.068	125	143.047	60.919			
115	155.204	135.867	123	145	55.714			
116	186.245	134.284	122.37	144.527	63.143			
117	186.245	133.065	115.667	139.855	63.143			
118	186.245	135.531	125.259	137.778	63.143			
119	217.286	138.727	123.481	145.269	74.286			
120	186.245	140.861	126.667	147	66.857			
121	194.005	136.982	124.444	142.333	66.857			
122	155.204	135.506	125.556	139.547	52.528			
123	186.245	132.528	124.333	136.657	63.143			
124	186.245	131.052	111.037	140.667	63.143			
125	201.765	130.207	116.667	137.049	70.571			
126	194.005	126.679	117.037	132.222	66.857			
127	186.245	133.355	122.111	139.546	63.143			
128	217.286	133.07	123.481	137.487	74.286			
129	194.005	132.364	124	137.333	66.857			
130	186.245	133.386	122.667	137.667	63.143			
131	170.724	132.731	123.667	137.004	58.138			
132	186.245	126.937	110.333	132.027	64.119			
133	186.245	121.284	110.333	126.333	63.143			
134	186.245	126.806	119	130.333	66.857			
135	225.046	121.923	105.778	126.556	78			
136	201.765	149.962	135.333	154.88	70.571			
137	217.286	146.448	136.778	152.519	74.286			
138	217.286	147.097	134	155.025	74.286			
139	186.245	147.154	137.074	151.884	63.143			
140	170.724	145.462	132.333	153.159	58.728			

141	201.765	141.282	131	147.641	68.488			
142	170.724	137.139	119.889	144.534	59.429			
143	194.005	138.76	126.852	144.926	66.857			
144	155.204	135.467	125	138.333	55.714			
145	194.005	139.664	130.815	144.778	66.857			
146	225.046	144.605	129	151.778	78			
147	217.286	140.761	130.259	147.955	74.379			
148	225.046	141.151	121.148	148.63	78			
149	194.005	138.664	129.63	146.663	66.443			
150	178.485	138.3	127.937	144.203	60.464			
151	155.204	137.348	121.778	142.251	52			
152	170.724	136.643	117.444	146.272	59.545			
153	194.005	132.141	116.519	138.741	66.857			
154	170.724	145.05	137	148.185	59.429			
155	201.765	148.453	137.074	154.8	70.571			
156	155.204	146.646	138.556	151.936	52			
157	170.724	145.855	137.778	151.333	59.429			
158	217.286	141.193	126.444	152.778	74.749			
159	170.724	142.447	132.519	148.112	58.728			
160	186.245	139.351	128.556	144.889	63.143			
161	186.245	138.767	123.778	145.565	63.143			
162	170.724	138.24	126.778	142.887	59.429			
163	194.005	134.902	124.444	139.333	66.857			
164	194.005	135.502	121.296	140.333	66.857			
165	217.286	131.813	117.593	136.436	74.286			
166	170.724	133.064	123.667	136.217	59.429			
167	170.724	128.467	121.556	136.172	58.019			
168	170.724	129.845	123.556	134.074	57.661			
169	217.286	120.056	105.095	128.951	74.286			
170	186.245	123.603	113	128.874	63.143			
171	201.765	118.184	109	123.28	70.571			
172	201.765	136.367	123.667	143.889	70.571			
173	170.724	139.669	128.222	143.333	59.429			
174	194.005	138.636	125	143.333	66.857			
175	170.724	137.493	124.889	142.185	59.429			
176	170.724	138.158	125.407	145.815	58.019			
177	217.286	129.356	114.667	140.444	74.286			
178	194.005	117.613	113.444	121.556	66.857			
179	201.765	130.215	114.444	138.667	70.571			
180	194.005	130.274	116.481	137.889	66.857			

181	201.765	140.427	127.519	145.015	70.571			
182	186.245	142.922	133.889	146.319	63.143			
183	186.245	137.771	126.889	141.802	63.143			
184	170.724	141.834	131.111	144.937	59.429			
185	209.526	133.648	120.667	145.519	71.349			
186	178.485	133.94	122.667	140.41	60.006			
187	162.964	135.815	121.889	141.333	55.714			
188	194.005	132.338	122	138.222	66.857			
189	186.245	131.343	114.63	140.377	63.143			
190	201.765	142.406	130.556	146.773	70.669			
191	217.286	144.558	127.741	151.37	74.286			
192	217.286	142.296	127	147.333	74.286			
193	225.046	139.465	126.926	145.852	78			
194	170.724	138.501	127.704	144.259	58.728			
195	178.485	136.901	122.333	144.432	61.258			
196	217.286	133.142	113.667	144.086	74.286			
197	186.245	135.394	121.37	140.092	63.143			
198	170.724	132.156	121.926	138.683	59.429			
199	201.765	138.048	125.111	144.139	70.669			
200	201.765	140.468	127.556	148.907	70.571			
201	170.724	140.937	129.333	146.19	59.429			
202	201.765	137.115	121.667	144.57	70.571			
203	178.485	139.077	128.889	143.505	60.006			
204	155.204	133.151	123.333	137.801	54.081			
205	170.724	133.74	118.222	141.238	59.429			
206	170.724	131.88	118.556	139.423	59.545			
207	201.765	126.773	109.222	135.271	70.669			
208	201.765	138.052	125.556	145.004	70.571			
209	217.286	139.635	126.148	144.362	74.379			
210	170.724	141.681	136.111	144.725	59.429			
211	201.765	137.302	128	142.4	70.571			
212	170.724	140.352	124.444	145.985	57.661			
213	186.245	131.455	126.222	137.072	64.867			
214	162.964	133.19	125.222	138.444	55.714			
215	170.724	132.028	118.556	136.889	59.429			
216	194.005	128.467	111.889	136.074	66.857			
217	170.724	135.42	127.556	140.148	59.429			
218	201.765	138.816	128	143.693	70.571			
219	194.005	134.409	124	141.778	66.857			
220	186.245	134.44	123.519	141.167	63.143			

221	155.204	135.276	126.667	141.852	53.568			
222	186.245	134.481	121.333	139.932	63.578			
223	201.765	128.417	110.667	139.098	70.571			
224	170.724	128.377	113.296	133.97	59.429			
225	194.005	123.982	106.222	132.111	66.857			
226	186.245	134.194	120.667	140.667	66.857			
227	201.765	138.821	121.185	147.594	70.571			
228	217.286	137.004	121.654	143.21	74.286			
229	194.005	136.991	124.333	142	66.857			
230	186.245	135.656	121.667	140.7	64.119			
231	162.964	132.157	118.222	139.667	56.574			
232	170.724	129.465	116.111	136.349	59.545			
233	186.245	127.028	114.556	134.043	63.143			
234	186.245	122.903	107.889	129.638	63.143			
235	194.005	137.502	124.667	141.333	66.857			
236	186.245	134.726	126.222	137.333	63.143			
237	201.765	134.819	122.778	142.719	70.571			
238	201.765	136.12	118.481	142.441	70.571			
239	178.485	132.442	121.889	138.442	60.919			
240	178.485	131.087	118.222	136.718	61.258			
241	201.765	129.027	113.333	140.84	70.571			
242	194.005	125.105	111.185	129.037	66.857			
243	186.245	121.703	112.889	129.884	63.143			
244	201.765	132.543	121.111	137.32	70.571			
245	162.964	136.868	125.222	141.667	55.714			
246	162.964	136.025	131.556	138.259	55.714			
247	217.286	132.612	121.074	137.606	74.286			
248	178.485	133.109	122.222	136.012	60.006			
249	162.964	129.886	122	133.693	56.574			
250	186.245	127.471	108.556	137.525	63.143			
251	194.005	124.548	109.037	130.63	66.857			
252	194.005	122.705	110.63	129.556	66.857			
253	217.286	137.015	124.519	140.962	74.286			
254	186.245	138.706	127.333	142.222	63.143			
255	186.245	138.644	122.259	143.314	63.143			
256	201.765	135.074	120.778	142.993	70.571			
257	194.005	133.449	116.444	140	67.779			
258	155.204	133.416	125.444	136.86	51.734			
259	194.005	129.093	109.926	137.741	66.96			
260	194.005	126.493	113	133.111	66.96			

261	170.724	129.3	114.333	133.894	59.429			
262	217.286	131.12	117.593	136.041	74.286			
263	186.245	135.681	122.667	139.333	66.857			
264	186.245	137.292	127.333	140.412	63.143			
265	201.765	133.996	124.407	140.102	70.669			
266	209.526	131.642	123.037	138.325	71.349			
267	186.245	128.598	118.556	131.367	63.252			
268	170.724	124.961	118.778	128.762	59.429			
269	194.005	125.467	116.778	131	66.857			
270	170.724	126.476	113.519	131.37	59.429			
271	201.765	130.977	124.222	135	70.571			
272	194.005	133.236	122.111	137.889	66.857			
273	194.005	131.582	117.778	137.926	66.857			
274	225.046	130.605	121.556	136.111	78			
275	217.286	131.118	114.852	137.284	74.286			
276	155.204	132.615	123.333	137.953	53.568			
277	186.245	132.768	119	138.072	64.119			
278	201.765	124.821	108.667	132.667	70.571			
279	201.765	123.514	106.667	129.471	70.571			
280	170.724	130.201	118.667	136.473	59.429			
281	201.765	136.084	126.741	140.231	70.571			
282	217.286	138.892	123.556	145.686	74.286			
283	201.765	136.406	125	142.43	70.571			
284	194.005	137.596	123.593	143.593	66.857			
285	209.526	135.699	122.111	142.801	72.974			
286	162.964	131.186	120	138.444	56.574			
287	194.005	130.969	111.444	139.778	66.857			
288	217.286	131.077	110.852	138.951	74.286			
289	194.005	126.867	112.111	134.444	66.857			
290	186.245	135.98	123.519	139.7	63.143			
291	201.765	138.793	122.778	146.111	70.571			
292	194.005	137.469	122.222	144.444	66.96			
293	162.964	139.666	129.333	145.267	55.838			
294	162.964	132.008	119.148	144	56.696			
295	170.724	132.814	121.111	141.937	59.429			
296	162.964	126.273	113	132.37	55.714			
297	162.964	126.265	118.111	132.667	55.714			
298	186.245	136.405	121.815	142.725	63.143			
299	186.245	138.097	123.333	143.667	66.857			
300	170.724	138.598	128.333	143.238	59.429			

301	201.765	136.85	125.519	142.535	70.571			
302	162.964	133.465	127.259	140.422	55.714			
303	194.005	133.391	123	138.667	66.857			
304	186.245	130.592	119.222	137.211	63.143			
305	170.724	128.165	118.926	133.259	59.429			
306	186.245	136.936	125	142.177	63.143			
307	217.286	137.439	126.667	141.556	74.286			
308	194.005	135.129	123.556	139.889	66.857			
309	170.724	134.952	127.519	138.882	59.429			
310	178.485	133.713	119.667	138.648	60.006			
311	162.964	130.617	118.111	134.556	56.818			
312	170.724	131.385	118	134.986	59.429			
313	186.245	130.671	120	134.855	63.143			
314	170.724	125.749	109.889	130	59.429			
315	217.286	134.011	123.556	137.54	74.286			
316	194.005	137.514	123.778	144.259	66.857			
317	194.005	139.196	127.778	144.333	66.857			
318	194.005	136.027	121	143	66.857			
319	186.245	135.83	127.778	142.464	64.867			
320	186.245	122.604	110.013	135.166	63.034			
321	186.245	129.76	112.037	135.181	63.252			
322	194.005	126.191	118.889	130.111	66.857			
323	194.005	125.475	111.667	134.741	66.96			
324	201.765	134.616	118.667	138.633	70.571			
325	217.286	137.787	119.889	143.001	74.286			
326	186.245	138.224	127.333	141.604	63.143			
327	186.245	137.215	123.704	142.567	63.143			
328	217.286	135.167	120.259	142.223	74.656			
329	170.724	132.522	121	142.458	59.891			
330	186.245	128.896	111.481	135.628	63.143			
331	194.005	128.067	111.889	134.333	66.857			
332	201.765	126.035	108.704	132.067	70.669			
333	194.005	133.293	124.444	136.667	66.857			
334	217.286	137.273	125.333	142.731	74.286			
335	186.245	136.223	122.074	141.333	63.143			
336	194.005	135.641	128.333	140.111	66.857			
337	217.286	133.298	119.556	140.809	74.286			
338	178.485	131.744	126	138.746	61.482			
339	217.286	128.673	112.926	136.444	74.286			
340	155.204	129.251	122	134.962	52.528			

341	162.964	126.122	112.222	131.111	55.714			
342	217.286	131.82	120	137	74.286			
343	170.724	139.698	131.667	144.799	59.429			
344	170.724	136.402	127.667	140.827	59.429			
345	201.765	135.651	123.963	144.222	70.571			
346	186.245	130.361	117.111	141.493	63.252			
347	155.204	134.276	124.889	140.76	52			
348	194.005	128.058	111	134	66.857			
349	162.964	130.205	120.074	135.148	55.714			
350	194.005	121.591	112.667	129.444	66.857			
351	194.005	133.354	118.333	142.815	66.857			
352	186.245	135.098	121	140.28	63.252			
353	194.005	132.867	126.222	135.593	66.857			
354	194.005	133.157	121	139.074	66.857			
355	194.005	129.386	117	139.519	66.131			
356	201.765	128.331	117	138.311	70.571			
357	194.005	125.778	112.926	130.444	66.857			
358	170.724	124.397	114	132.667	59.429			
359	194.005	122.701	112.593	129.556	66.857			

Bin	*Frequency*
40	0
45	0
50	0
55	18
60	89
65	76
70	74
75	91
80	11
More	0

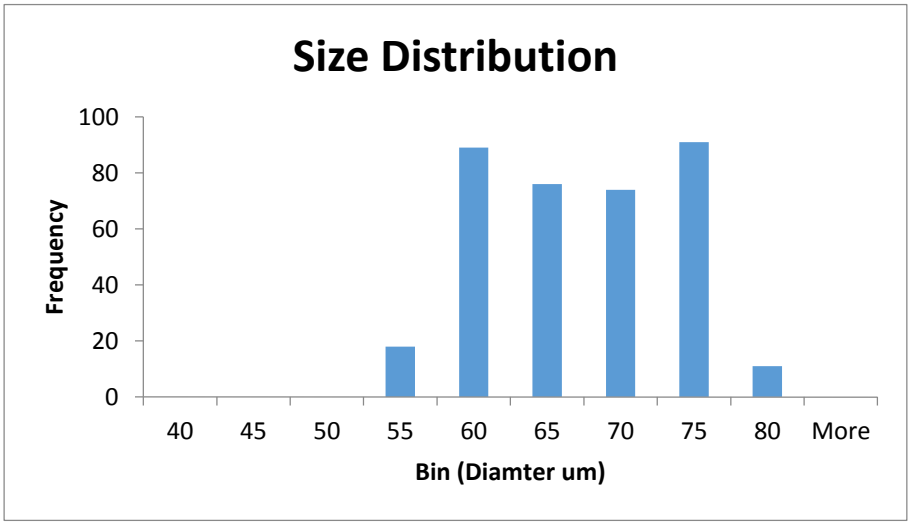

Appendix C: ABET Requirements

3. An ability to design a system, component, or process to meet desired needs within realistic constraints such as economic, environmental, social, political, ethical, health and safety, manufacturability, and sustainability (ABET 3c) while incorporating appropriate engineering standards (ABET Criterion 5) (need to assess each of these separately, but since 'or' and "such as" not all need to be met separately).
    - i) multiple realistic constraints (economic, environmental, social, political, ethical, health and safety, manufacturability) – **pages 33-34, 50-52**
    - ii) appropriate engineering standards **- pages 36-47**
4. An ability to function on multidisciplinary teams (3d). **pages 6-7**
6. An understanding of professional and ethical responsibilities (3f)
    - i) Professional – **pages 7, 50-52**
    - ii) Ethical – **pages 12**
7. An ability to communicate effectively (3g). **pages 1-75**
8. The broad education necessary to understand the impact of engineering solutions in a global, economic, environmental, and societal context (3h). (both economic AND environmental need to be addressed)
    - i) Economic – **pages 50-52**
    - ii) Environmental – **pages 50-52**
10. A knowledge of contemporary issues (3j). **pages 9-12**